Gravitational perturbations and metric reconstruction: Method of extended homogeneous solutions applied to eccentric orbits on a Schwarzschild black hole

Seth Hopper[*] and Charles R. Evans[†]

Department of Physics and Astronomy, University of North Carolina, Chapel Hill, North Carolina 27599

We calculate the gravitational perturbations produced by a small mass in eccentric orbit about a much more massive Schwarzschild black hole and use the numerically computed perturbations to solve for the metric. The calculations are initially made in the frequency domain and provide Fourier-harmonic modes for the gauge-invariant master functions that satisfy inhomogeneous versions of the Regge-Wheeler and Zerilli equations. These gravitational master equations have specific singular sources containing both delta function and derivative-of-delta function terms. We demonstrate in this paper successful application of the method of extended homogeneous solutions, developed recently by Barack, Ori, and Sago, to handle source terms of this type. The method allows transformation back to the time domain, with exponential convergence of the partial mode sums that represent the field. This rapid convergence holds even in the region of r traversed by the point mass and includes the time-dependent location of the point mass itself. We present numerical results of mode calculations for certain orbital parameters, including highly accurate energy and angular momentum fluxes at infinity and at the black hole event horizon. We then address the issue of reconstructing the metric perturbation amplitudes from the master functions, the latter being weak solutions of a particular form to the wave equations. The spherical harmonic amplitudes that represent the metric in Regge-Wheeler gauge can themselves be viewed as weak solutions. They are in general a combination of (1) two differentiable solutions that adjoin at the instantaneous location of the point mass (a result that has order of continuity C^{-1} typically) and (2) (in some cases) a delta function distribution term with a computable time-dependent amplitude.

PACS numbers: 04.25.dg, 04.30.-w, 04.25.Nx, 04.30.Db

I. INTRODUCTION

Considerable research on the two-body problem in general relativity has been fostered over the past decade by the prospects of detecting gravitational radiation from extreme-mass-ratio binaries. The general relativistic two-body problem is notoriously difficult, as it involves dynamics of the motion of the bodies and of the gravitational field itself. Gravitational wave emission carries away energy and angular momentum from the orbit, leading to inspiral and eventual merger. The future joint NASA-ESA LISA mission [1] is expected to detect between tens and thousands of such extreme-mass-ratio inspirals (EMRIs)–binaries composed of a compact object ($\mu \sim 1 - 50 M_\odot$) in orbit about a supermassive Kerr black hole ($M \sim 10^5 - 10^7 M_\odot$) out to cosmological distances ($z \sim 1$) [2]. The small mass ratio $10^{-7} \lesssim \mu/M \lesssim 10^{-3}$ of expected astrophysical sources [3] implies a gradual change in orbital parameters, with $\gtrsim 10^5$ wave periods as the binary evolves through the LISA passband ($10^{-4} - 10^{-2}$ Hz). Detailed theoretical calculations will aid in both detection of EMRI gravitational wave signals and in determination of the source's physical parameters.

Quite apart from the prospects of astrophysical observation, this problem is one of intrinsic interest in theoretical physics. Of the various possibilities, the physically simplest compact binary is one composed of two black holes. Such a system eliminates the complications of stellar microphysics and reduces the problem to a minimum parameter set. In approaching the problem mathematically, the extreme mass-ratio and gradual orbital evolution is of benefit theoretically, allowing black hole perturbation theory to be used. Furthermore, the small mass ratio allows even the black hole structure of the small mass to be ignored (at lowest order), restoring a point-like (particle) behavior [4] on length scales that are large compared to μ and thereby simplifying the perturbation problem.

The perturbation problem proceeds in stages. At the outset the motion of the particle is taken as a geodesic ($\mu/M \to 0$, or zeroth order) on the background spacetime. The first-order (in μ/M) gravitational field perturbation is then computed, yielding a new metric $\mathrm{g}_{\mu\nu} = g_{\mu\nu} + p_{\mu\nu}$ that corrects the background metric $g_{\mu\nu}$. The gravitational waves in the perturbation $p_{\mu\nu}$ carry energy and angular momentum to infinity and down the black hole event horizon, giving rise to a back reaction or local self-force (SF) on the particle that has both conservative and dissipative terms.

---

[*]Electronic address: hoppese@physics.unc.edu
[†]Electronic address: evans@physics.unc.edu

Formally, the SF depends on gradients of $p_{\mu\nu}$ and acts locally on the particle to accelerate it off its background geodesic. Once the first-order correction to the motion is successfully computed, the calculation may proceed to second order in the field perturbation (see Pound [5] for a recent background discussion and an alternative formulation).

Yet having idealized the small body as a point particle, the metric perturbation and SF are found to diverge at the location of the particle, and the formal perturbation to the equation of motion is meaningless without careful regularization. This problem is similar to the classic SF problem of an accelerating, radiating charge in electromagnetic theory in flat spacetime [6]. Two pivotal papers, by Mino, Sasaki, and Tanaka [7] and Quinn and Wald [8], showed how the metric perturbation may be separated into a divergent, direct part $p_{\mu\nu}^{\rm dir}$ and a finite tail term $p_{\mu\nu}^{\rm tail}$, with the latter providing the regularized field that makes the SF finite. As an alternative, Detweiler and Whiting [9] proposed decomposing the metric perturbation into regular $p_{\mu\nu}^{R}$ and singular $p_{\mu\nu}^{S}$ parts. Under this interpretation, $p_{\mu\nu}^{R}$ is a solution to the vacuum field equations, but gives rise to the same SF as $p_{\mu\nu}^{\rm tail}$.

Since then, SF calculations have been made in certain special cases [10–14]. See the review by Barack [2]. Ultimately, the theory aims to provide self-consistent SF calculations of arbitrary orbits about Kerr black holes. In this paper, we concern ourselves with a more modest goal: demonstrating a complete computation of the radiative gravitational perturbations produced by a mass in eccentric orbit on a Schwarzschild black hole and reconstruction of the corresponding parts of the perturbed metric in Regge-Wheeler gauge. While we leave for another occasion computation of both the nonradiative perturbations and the SF, the accurate reconstruction of the radiative parts of the metric, at all locations up to and including the point mass, should serve as a starting point for a further gauge transformation or alternative regularization technique.

We note in passing that most work to date computing EMRI evolution has not made use of local SF calculation. Sufficiently adiabatic changes in an orbit on Schwarzschild spacetime allow a *balance calculation* approach [15], where orbital energy and angular momentum are "evolved" (acausally) to match corresponding gravitational wave fluxes through bounding surfaces at large radius and near the horizon. Much effort is ongoing to extend the reach of adiabatic calculations [16–18]. Unfortunately, the approach only approximates dissipative SF terms and cannot account for conservative SF effects. In any event, the more self-consistent SF approach should serve to confirm the validity of these or other approximations.

Perturbation theory for Schwarzschild black holes has a traditional formalism pioneered by Regge and Wheeler [19], Zerilli [20], and Vishveshwara [21] that uses spherical harmonics and the Regge-Wheeler gauge to simplify algebraically the form of the metric perturbation. At each spherical harmonic order there are just two *master* functions, $\Psi_{\ell m}^{\rm even}(t,r)$ and $\Psi_{\ell m}^{\rm odd}(t,r)$, one for each parity or gravitational degree of freedom, which satisfy linear inhomogeneous wave equations in t and r. The formalism was improved by Moncrief [22] and colleagues [23, 24], making use instead of gauge-invariant master functions that satisfy similar wave equations. Recently Martel and Poisson [25] have placed the theory in both a gauge-invariant and covariant form.

For perturbations of Kerr black holes, Teukolsky [26] developed a formalism based on Newman-Penrose curvature scalars and spin-weighted spheroidal harmonics. In the frequency domain the radial part is a single (complex) master equation [27], which can, of course, be applied to a Schwarzschild hole as well [15, 28].

An alternative to the Regge-Wheeler-Zerilli (RWZ) approach has recently been advanced by Barack and Lousto [29]. They propose directly evolving the ten spherical harmonic amplitudes that describe the metric perturbation in Lorenz (or harmonic) gauge. In this direct metric perturbation approach, the equations separate into even- and odd-parity sectors, yet still involve systems of seven and three coupled equations, respectively. Barack and Sago [11, 14] have used the formalism to compute the time evolution of metric perturbations generated by circular and eccentric orbits on Schwarzschild, along with the resulting SF components.

The RWZ and direct metric perturbation approaches each have advantages and disadvantages. The direct metric perturbation formalism yields directly what one wants as an input to a SF calculation, namely the metric itself in Lorenz gauge. In a time domain calculation, as so far employed, it has the disadvantage of requiring simultaneous solution of a large set of coupled partial differential equations (PDE's). Anticipating the subtraction involved in the SF regularization, Barack, Lousto, and Sago have built a fourth-order convergent finite difference code to compute the modes to sufficient accuracy. In contrast, the RWZ approach has the advantage that only a single uncoupled wave equation need be solved for each mode and parity. Unfortunately, an added step is required to reconstruct the metric from the mode solutions. Moreover, the reconstruction involves terms that are singular at the particle location and the simplest reconstruction yields the metric perturbation in Regge-Wheeler gauge [30, 31]. Finally, the RWZ approach provides only the radiative ($\ell \geq 2$) parts of the perturbation and the nonradiative modes ($\ell = 0, 1$) must be derived by separate means.

In this paper we opt for using the gauge-invariant RWZ approach detailed by Martel and Poisson [25], and adopt the Zerilli-Moncrief $\Psi_{\ell m}^{\rm ZM} = \Psi_{\ell m}^{\rm even}$ and Cunningham-Price-Moncrief $\Psi_{\ell m}^{\rm CPM} = \Psi_{\ell m}^{\rm odd}$ master functions for even and odd-parity, respectively. Our use of this relatively standard method is augmented, though, by a new technique that enables accurate reconstruction of the corresponding parts of the metric in Regge-Wheeler gauge. We leave for a later occasion our own consideration of the monopole and dipole terms (which are essential to a SF calculation) and

instead direct attention to discussion by Detweiler and Poisson [32] and recent successful numerical implementation by Barack and Sago [14].

The master functions can be obtained directly by numerical evolution (solution of PDE's) in the time domain (TD) (see e.g., [10, 11, 13, 14, 30, 33–35]) or by numerical integration of ordinary differential equations (ODE's) for the Fourier modes in the frequency domain (FD) (see e.g., [15, 36–38]). Each method has strengths and weaknesses. TD calculations require solving just one equation for each ℓ, m mode and time dependence of the subsequently reconstructed metric and SF is of direct interest. Disadvantages of TD calculations include (1) modeling the discontinuous source movement through the finite difference grid [14, 29]; (2) numerical stability of PDE evolution; (3) difficulty devising numerical schemes of adequately small truncation error; and (4) challenges in posing outgoing wave boundary conditions at finite radius. In contrast, in FD calculations (1) the numerical errors tend to be much smaller (i.e., by solving ODE's); (2) outgoing wave boundary conditions are handled mode-by-mode and extrapolated to infinity and to the black hole event horizon; and (3) the discontinuous source presents few difficulties in computing (at least) the Fourier mode functions $R_{\ell mn}(r)$. However, FD methods require, for eccentric orbits, computing and summing over numerous harmonics n of the radial libration frequency Ω_r for each ℓ, m and transformation to the TD is nontrivial given the singular source terms.

Barack, Ori, and Sago (BOS) [38] highlighted the latter difficulty. They used the model problem of a scalar field $\Phi(t, r, \theta, \varphi)$ generated by a scalar point charge in eccentric orbit on Schwarzschild. The spherical harmonic modes $\phi_{\ell m}(t, r) = r\Phi_{\ell m}(t, r)$ satisfy a wave equation with a singular source, $S_{\ell m}^{\text{scalar}}(t, r) = C_{\ell m}(t, r)\,\delta[r - r_p(t)]$. Here $C_{\ell m}(t, r)$ is some smooth function and $r = r_p(t)$ describes the radial libration of the particle's worldline between two turning points. In the FD, ODE's are solved for the Fourier-harmonic modes $R_{\ell mn}(r)$. These mode functions are, at each point r, Fourier series coefficients. The resulting Fourier series converges for the piecewise continuous (C^0) $\phi_{\ell m}(t, r)$ but the singular nature of the source S makes $\phi_{\ell m}(t, r)$ converge slowly in the region traversed by the point charge. The radial derivative $\partial_r \phi_{\ell m}$ is however discontinuous at $r = r_p(t)$ and its Fourier series only converges, in the usual sense [39], almost everywhere. The attempt to assemble the radial derivative from the Fourier series is plagued by the Gibbs phenomenon; the series converges to the mean value at the discontinuity and the series "overshoots" and fails to converge properly in the limit as both $n \to \infty$ and $r \to r_p(t)^{\pm}$.

BOS circumvented the difficulty with a new *method of extended homogeneous solutions*. In brief, they use FD analysis to find Fourier-harmonic mode solutions to the homogeneous equation, valid outside and on either side of the source libration region. The associated Fourier series converge exponentially fast to homogeneous solutions of the TD wave equation. They then analytically extend both homogeneous TD solutions into the source libration region up to the instantaneous position of the point charge. Summed to adequately high order, the two homogeneous solutions match in value at $r_p(t)$, as expected. With the field represented in this way, the left and right derivatives can be accurately determined. BOS argued that the method should work for other problems with similar wave equations, including the Teukolsky equation.

We show in this paper that the method can indeed be extended to the case of gravitational perturbations computed in the RWZ formalism, and apply the method to a large set of Fourier-harmonic modes stemming from a mass in eccentric orbit on Schwarzschild. (Note that Barack and Sago [14] previously implemented this method in the gravitational case but only for the $\ell = 0, 1$ modes in Lorenz gauge.) An important distinction arises: in the gravitational case the source distribution in the Regge-Wheeler gauge contains both delta function and derivative-of-delta function terms,

$$S_{\ell m}(t, r) = G_{\ell m}(t, r)\,\delta[r - r_p(t)] + F_{\ell m}(t, r)\,\delta'[r - r_p(t)], \tag{1.1}$$

with $G_{\ell m}(t, r)$ and $F_{\ell m}(t, r)$ being smooth functions. As a consequence the master functions have a jump discontinuity at $r = r_p(t)$ (referred to sometimes as a C^{-1} function). The resulting extension of the homogeneous solutions, $\Psi_{\ell m}^+$ and $\Psi_{\ell m}^-$, written as

$$\Psi_{\ell m}(t, r) = \Psi_{\ell m}^+(t, r)\,\theta[r - r_p(t)] + \Psi_{\ell m}^-(t, r)\,\theta[r_p(t) - r], \tag{1.2}$$

where $\theta[r - r_p(t)]$ is the Heaviside function, is a type of *weak solution* to the inhomogeneous master equation. Thus in the gravitational case in RWZ gauge the difficulty with local convergence occurs with the master function itself. We show that the use of distributions, or generalized functions [40], makes possible separate analytic calculation of the expected jumps in value and slope of $\Psi_{\ell m}$. We further demonstrate that the metric perturbation can be accurately numerically computed, including the time dependent magnitudes of delta function terms that appear in some of the metric amplitudes in Regge-Wheeler gauge.

This paper is organized as follows. In Sec. II we briefly outline the general mathematical problem of using FD techniques to solve for perturbations in the RWZ formalism. We also review the standard parameterization of eccentric orbits. Sec. III concerns the method of extended homogeneous solutions. We first review BOS's solution for the scalar field case. We show then our treatment of more general source terms and extension of the method to gravitational perturbations. Sec. IV provides numerical results on the computed Fourier-harmonic mode functions, including

convergence tests and calculation of radiated gravitational wave energy and angular momentum. In particular, the energy and angular momentum fluxes are shown to agree with past published values. More importantly, the method is shown to provide a solution to the field and its derivatives that is convergent exponentially fast everywhere. Then in Sec. V, we show that the equations which allow the metric to be obtained from the master functions, along with an understanding of the form of the weak solutions for $\Psi_{\ell m}^{\text{even}}$ and $\Psi_{\ell m}^{\text{odd}}$, can be used to determine both the smooth and distributional parts of the metric. App. A discusses fully evaluated forms of distributional source terms. App. B gives the details of such source terms for our case of eccentric orbits on Schwarzschild. In App. C we concisely summarize the metric perturbation formalism in the Regge-Wheeler gauge. We show the construction of gauge-invariant master functions of each parity, and provide the spherical harmonic decomposition of the Einstein equations and Bianchi identities. App. D concludes this paper with a brief discussion of asymptotic expansions used to set boundary conditions on the mode functions at large r.

Throughout this paper we use the sign conventions and notation of Misner, Thorne, and Wheeler [41] and use units in which $c = G = 1$. We use Schwarzschild coordinates $x^\mu = (t, r, \theta, \varphi)$ except as otherwise indicated.

II. BACKGROUND ON THE STANDARD RWZ APPROACH TO GRAVITATIONAL PERTURBATIONS IN THE FREQUENCY DOMAIN

In this section we briefly summarize both the standard notation for parameterizing bound orbits on Schwarzschild and the usual approach to computing gravitational perturbations using the Regge-Wheeler-Zerilli (RWZ) formalism in the frequency domain (FD). The description of the geodesic motion on the background, in terms of various curve functions, is used throughout the rest of the paper. The standard FD analysis provides the notation for describing the Fourier-harmonic modes, and their normalization, and sets the stage for discussion in Sec. III of how gravitational perturbations can be returned successfully to the time domain (TD). Here, and throughout this paper, we use a subscript p to indicate evaluation along the worldline of the particle.

A. Bound orbits on a Schwarzschild black hole

Consider bound timelike geodesic motion around a Schwarzschild black hole (i.e., $\mu \to 0$). We may for the nonce use proper time τ to parameterize the geodesic, $x_p^\mu(\tau) = [t_p(\tau), r_p(\tau), \theta_p(\tau), \varphi_p(\tau)]$, with the associated four-velocity $u^\mu = dx_p^\mu/d\tau$. On Schwarzschild we take $\theta_p(\tau) = \pi/2$ without loss of generality. The geodesic equations yield immediate first integrals and allow the trajectory to be described by the conserved energy $\mathcal{E}$ and angular momentum $\mathcal{L}$ per unit mass. Alternatively, we can choose the (dimensionless) semi-latus rectum p and the eccentricity e as orbital parameters (c.f., [14, 15]). A third choice would be use of the periapsis and apapsis, $r_{\min}$ and $r_{\max}$. We will find all of these useful in what follows. The latter two parameter pairs are related to each other by

$$p \equiv \frac{2r_{\max}r_{\min}}{M(r_{\max} + r_{\min})}, \qquad e \equiv \frac{r_{\max} - r_{\min}}{r_{\max} + r_{\min}}, \tag{2.1}$$

or inversely

$$r_{\max} = \frac{pM}{1 - e}, \qquad r_{\min} = \frac{pM}{1 + e}. \tag{2.2}$$

The specific energy and angular momentum are related to p and e by [15]

$$\mathcal{E}^2 = \frac{(p - 2 - 2e)(p - 2 + 2e)}{p(p - 3 - e^2)}, \qquad \mathcal{L}^2 = \frac{p^2 M^2}{p - 3 - e^2}. \tag{2.3}$$

The geodesic equations provide the following differential equations for the orbital motion and for the time dependence of the four-velocity,

$$\frac{dt_p}{d\tau} = u^t = \frac{\mathcal{E}}{f_p}, \qquad \frac{d\varphi_p}{d\tau} = u^\varphi = \frac{\mathcal{L}}{r_p^2}, \qquad \left(\frac{dr_p}{d\tau}\right)^2 = (u^r)^2 = \mathcal{E}^2 - U_p^2, \tag{2.4}$$

where

$$f(r) \equiv 1 - \frac{2M}{r}, \qquad U^2(r, \mathcal{L}^2) \equiv f\left(1 + \frac{\mathcal{L}^2}{r^2}\right). \tag{2.5}$$

For purposes of numerical integration there is another curve parameter, originally devised by Darwin [42], that proves useful. Here one introduces a phase angle χ that is related to the radial position on the orbit by the Keplerian-appearing form

$$r_p\left(\chi\right) = \frac{pM}{1 + e\cos\chi}.$$ (2.6)

Of course, in the relativistic case χ differs from the true anomaly φ. The orbit goes through one radial libration for each change $\Delta\chi = 2\pi$. The use of χ eliminates singularities in the differential equations at the turning points [15]. Note that at $\chi = 0$, $r_p = r_{\min}$ and at $\chi = \pi$, $r_p = r_{\max}$. (Also note that in this section we are content with making a slight abuse of notation in jumping from $r_p(\tau)$ to $r_p(\chi)$, before ultimately settling on $r_p(t)$.) In terms of χ the equations are

$$\frac{dt_p}{d\chi} = \frac{p^2 M}{(p - 2 - 2e\cos\chi)(1 + e\cos\chi)^2}\left[\frac{(p-2)^2 - 4e^2}{p - 6 - 2e\cos\chi}\right]^{1/2},$$ (2.7)

$$\frac{d\varphi_p}{d\chi} = \left[\frac{p}{p - 6 - 2e\cos\chi}\right]^{1/2},$$ (2.8)

and

$$\frac{d\tau_p}{d\chi} = \frac{Mp^{3/2}}{(1 + e\cos\chi)^2}\left[\frac{p - 3 - e^2}{p - 6 - 2e\cos\chi}\right]^{1/2}.$$ (2.9)

We use Eq. (2.7) to derive the fundamental frequency and period of radial motion,

$$\Omega_r \equiv \frac{2\pi}{T_r}, \qquad T_r \equiv \int_0^{2\pi}\left(\frac{dt_p}{d\chi}\right)d\chi.$$ (2.10)

It is also of importance to have the average rate at which the azimuthal angle advances, found by averaging the angular frequency $d\varphi_p/dt$ over a radial libration via

$$\Omega_\varphi \equiv \frac{1}{T_r}\int_0^{T_r}\left(\frac{d\varphi_p}{dt}\right)dt.$$ (2.11)

While T_r represents the lapse of coordinate time in a radial libration, the time $T_\varphi = 2\pi/\Omega_\varphi$ has no particular physical significance [43]. Finally, because wave equation source functions contain terms like $\delta[r - r_p(t)]$ and $\delta'[r - r_p(t)]$, we have need of derivatives of $r_p(t)$,

$$\dot{r}_p^2(t) = f_p^2 - \frac{f_p^2}{\mathcal{E}^2}U_p^2, \qquad \ddot{r}_p(t) = \frac{2Mf_p}{r_p^2} - \frac{f_p^2}{\mathcal{E}^2 r_p^2}\left[3M - \frac{\mathcal{L}^2}{r_p} + \frac{5M\mathcal{L}^2}{r_p^2}\right],$$ (2.12)

where we let a dot signify differentiation with respect to coordinate time.

B.   The Regge-Wheeler-Zerilli formalism in the frequency domain

As discussed in the Introduction, we use the RWZ approach to gravitational perturbations and use specifically the even-parity Zerilli-Moncrief function $\Psi_{\ell m}^{\mathrm{even}}$ [22] and the odd-parity Cunningham-Price-Moncrief function $\Psi_{\ell m}^{\mathrm{odd}}$ [24]. See Martel and Poisson [25] for recent discussion and references therein. Both of these functions satisfy wave equations of the form

$$\left[-\frac{\partial^2}{\partial t^2} + \frac{\partial^2}{\partial r_*^2} - V_\ell(r)\right]\Psi_{\ell m}(t, r) = S_{\ell m}(t, r),$$ (2.13)

where $r_* = r + 2M\ln(r/2M - 1)$ is the usual tortoise coordinate. The potential used in Eq. (2.13) is either the Zerilli or Regge-Wheeler potential depending on whether the parity is even or odd, respectively.

The source terms also depend upon parity but further depend on which specific master functions are chosen. Martel and Poisson gave the covariant form of $S_{\ell m}^{\mathrm{even}}$ and $S_{\ell m}^{\mathrm{odd}}$ (see App. C for these in Schwarzschild coordinates) that are

associated with the Zerilli-Moncrief and Cunningham-Price-Moncrief functions. Martel [30] derived the detailed form of $S_{\ell m}^{\mathrm{even}}$ for a point mass in eccentric orbit. Sopuerta and Laguna [35] derived the detailed form of $S_{\ell m}^{\mathrm{odd}}$ for eccentric orbits (see also Field et al. [44]). We give in App. B detailed expressions for these sources in a form that is useful for both mode integrations and metric reconstruction.

In each case the source term has the following general form

$$S_{\ell m}(t, r) = \tilde{G}_{\ell m}(t)\, \delta[r - r_p(t)] + \tilde{F}_{\ell m}(t)\, \delta'[r - r_p(t)], \tag{2.14}$$

where $\tilde{G}_{\ell m}(t)$ and $\tilde{F}_{\ell m}(t)$ are smooth (differentiable) functions. Note that the source, as written here, differs from notation originally used by Martel [30] (who retained smooth functions of r and t, as in Eq. (1.1)). Our expression uses the delta function, and parts integration, to yield a *fully evaluated form* along the worldline of the particle (see App. A), making $\tilde{G}_{\ell m}(t)$ and $\tilde{F}_{\ell m}(t)$ unique functions of time only.

Eq. (2.13) can be solved directly in the TD–an approach that has received much attention lately. In this paper we are interested instead in extending the reach of FD analysis, and the balance of this section provides a brief review of the standard FD solution. We note in passing that a hybrid approach is possible–using FD analysis for low ℓ and m modes while using TD calculation for high order modes [45].

On Schwarzschild, eccentric orbits are typically not closed and therefore the motion is not simply periodic as seen by an asymptotic static observer. The radial libration is periodic (but not typically sinusoidal) with fundamental frequency Ω_r. The smooth functions $\tilde{G}_{\ell m}(t)$ and $\tilde{F}_{\ell m}(t)$, which depend upon the particle's radial and angular motion, have terms that are periodic with fundamental frequency Ω_r, but also involve a term that is proportional to $\exp[-im\varphi_p(t)]$. This latter term comes from restricting the spherical harmonics $Y_{\ell m}^*(\theta, \varphi)$ with $\delta[\varphi - \varphi_p(t)]$. The function $\varphi_p(t)$ advances with an average rate Ω_φ, but is modulated (in an eccentric orbit) by a function $\Delta\varphi(t)$ that is periodic with fundamental frequency Ω_r. Hence, the source $S_{\ell m}(t, r)$, and therefore the field $\Psi_{\ell m}(t, r)$, can be represented by a Fourier series with fundamental frequency Ω_r, but multiplied by a phase factor that advances linearly with rate Ω_φ. These fields *would* appear simply periodic to an observer whose frame rotates at rate Ω_φ [15]. To a static observer, a given mode ℓ and m will have a spectrum of harmonics offset by $m\Omega_\varphi$; taken together the full field will have a two-fold countably infinite frequency spectrum,

$$\omega = \omega_{mn} \equiv m\Omega_\varphi + n\Omega_r, \qquad m, n \in \mathbb{Z}. \tag{2.15}$$

Accordingly, the wave equation (2.13) Fourier transforms into a set of ODE's,

$$\left[\frac{d^2}{dr_*^2} - V_\ell(r) + \omega_{mn}^2\right] R_{\ell mn}(r) = Z_{\ell mn}(r), \tag{2.16}$$

where $R_{\ell mn}(r)$ and $Z_{\ell mn}(r)$ are Fourier harmonic amplitudes

$$R_{\ell mn}(r) \equiv \frac{1}{T_r} \int_0^{T_r} dt\, \Psi_{\ell m}(t, r)\, e^{i\omega_{mn}t}, \qquad Z_{\ell mn}(r) \equiv \frac{1}{T_r} \int_0^{T_r} dt\, S_{\ell m}(t, r)\, e^{i\omega_{mn}t}. \tag{2.17}$$

The series representations of $\Psi_{\ell m}(t, r)$ and $S_{\ell m}(t, r)$ are

$$\Psi_{\ell m}(t, r) = \sum_{n=-\infty}^{\infty} R_{\ell mn}(r)\, e^{-i\omega_{mn}t}, \qquad S_{\ell m}(t, r) = \sum_{n=-\infty}^{\infty} Z_{\ell mn}(r)\, e^{-i\omega_{mn}t}, \tag{2.18}$$

and are subject to the usual provisos of Fourier theory regarding for what r Eqs. (2.18) converge to the original functions.

In order to find the solution to Eq. (2.16), we start by solving the homogeneous version of that equation, obtaining two independent solutions. Using the terminology of Galt'sov [46] (see also [47] for a clear presentation of basis modes), the $R_{\ell mn}^-(r)$ solution is computed by setting a unit normalized "in" wave boundary condition of

$$\hat{R}_{\ell mn}^-(r_* \to -\infty) = e^{-i\omega_{mn}r_*}, \tag{2.19}$$

near the horizon. Similarly, the $R_{\ell mn}^+(r)$ solution arises from setting a unit normalized "up" boundary condition of

$$\hat{R}_{\ell mn}^+(r_* \to +\infty) = e^{i\omega_{mn}r_*}, \tag{2.20}$$

at large r_*. Formally, these homogeneous solutions are both valid in the entire range $2M < r < \infty$. The standard method of integrating the Green function and source (the method of variation of parameters) gives the solution to the inhomogeneous equation (2.16),

$$R_{\ell mn}(r) = c_{\ell mn}^+(r)\hat{R}_{\ell mn}^+(r) + c_{\ell mn}^-(r)\hat{R}_{\ell mn}^-(r), \tag{2.21}$$

where

$$c_{\ell mn}^+(r) \equiv \frac{1}{W_{\ell mn}} \int_{r_{\min}}^r dr' \frac{\hat{R}_{\ell mn}^-(r')Z_{\ell mn}(r')}{f(r')}, \qquad c_{\ell mn}^-(r) \equiv \frac{1}{W_{\ell mn}} \int_r^{r_{\max}} dr' \frac{\hat{R}_{\ell mn}^+(r')Z_{\ell mn}(r')}{f(r')}, \tag{2.22}$$

and

$$W_{\ell mn} \equiv \hat{R}_{\ell mn}^- \frac{d\hat{R}_{\ell mn}^+}{dr_*} - \hat{R}_{\ell mn}^+ \frac{d\hat{R}_{\ell mn}^-}{dr_*}, \tag{2.23}$$

is the Wronskian. Outside the source libration region, Eq. (2.21) reduces to the normalized homogeneous solutions that are properly connected through the source region,

$$\begin{aligned}
R_{\ell mn}^+(r) &= C_{\ell mn}^+ \hat{R}_{\ell mn}^+(r), \quad r \geq r_{\max}, \\
R_{\ell mn}^-(r) &= C_{\ell mn}^- \hat{R}_{\ell mn}^-(r), \quad r \leq r_{\min},
\end{aligned} \tag{2.24}$$

where $C_{\ell mn}^\pm$ are the values of $c_{\ell mn}^\pm(r)$ evaluated at the ends of the range of the source,

$$C_{\ell mn}^+ \equiv c_{\ell mn}^+(r_{\max}), \qquad C_{\ell mn}^- \equiv c_{\ell mn}^-(r_{\min}). \tag{2.25}$$

III. THE METHOD OF EXTENDED HOMOGENEOUS SOLUTIONS IN THE GRAVITATIONAL CASE

A. Brief review of Barack, Ori, and Sago's method of extended homogeneous solutions

As a model problem, Barack, Ori, and Sago (BOS) considered the scalar field Φ produced by a scalar point charge in an eccentric orbit on a Schwarzschild background. The spherical harmonic amplitudes $\phi_{\ell m}(t,r) = r\Phi_{\ell m}(t,r)$ of the scalar field satisfy RWZ-like equations fully analogous to Eq. (2.13) but with source functions that only depend upon a Dirac delta function,

$$S_{\ell m}^{\text{scalar}} = C_{\ell m}(t,r)\,\delta[r - r_p(t)]. \tag{3.1}$$

Here $C_{\ell m}(t,r)$ is a smooth function that is derived from the particle's point-like charge density ρ.

With a delta function source the amplitudes $\phi_{\ell m}(t,r)$ are left piecewise continuous (C^0) at the instantaneous particle location $r_p(t)$ but lose all differentiability there. BOS argued that this behavior, while surmountable in TD calculations, would cause difficulties for Fourier synthesis in FD calculations. As they convincingly demonstrated with their first two figures, while $\phi_{\ell m}(t,r)$ converges exponentially fast outside the radial libration region, the Gibbs phenomenon is responsible for a very slow convergence of $\phi_{\ell m}(t,r)$ between $r_{\min}$ and $r_{\max}$. Furthermore, the radial derivative $\partial_r \phi_{\ell m}$ is discontinuous at $r_p(t)$ and suffers the full effects of the Gibbs phenomenon–the Fourier series converges to the mean value at the discontinuity and partial sums ($-N \leq n \leq N$) overshoot in the limit as both $N \to \infty$ and $r \to r_p(t)^\pm$. This behavior is a serious obstacle to straightforward use of FD calculations in SF regularization.

As a solution to this problem, BOS developed the method of extended homogeneous solutions (EHS). Their method involves using the Fourier-harmonic modes of the homogeneous equation in the FD to synthesize homogeneous solutions $\phi_{\ell m}^-(t,r)$ and $\phi_{\ell m}^+(t,r)$ to the TD wave equation. The Fourier convergence of these homogeneous solutions is exponentially rapid. While these solutions exist in the entire radial domain ($2M < r < \infty$), ordinarily $\phi_{\ell m}^-(t,r)$ and $\phi_{\ell m}^+(t,r)$ would be viewed as meaningful in their respective source-free regions, $r < r_{\min}$ and $r > r_{\max}$. The heart of the BOS method lies in extending both of these solutions into the region of radial libration up to the instantaneous position of the particle.

BOS demonstrated the method numerically using the monopole term of Φ. A key condition for success of the method is that, as $N \to \infty$ in the partial sums, one finds

$$\lim_{r \to r_p(t)} \phi_{\ell m}^-(t,r) = \lim_{r \to r_p(t)} \phi_{\ell m}^+(t,r), \tag{3.2}$$

as expected analytically. This was observed numerically and the method as a whole converges rapidly since the FD solution of the inhomogeneous equation is never summed. BOS went on to argue that the method could be extended to any ℓ and m for scalar, electromagnetic, or gravitational fields.

B. Application to gravitational perturbations

In this section we detail our application of the method to the gravitational case in RWZ gauge. It is worth first observing the magnitude of the problem to be circumvented. Given the gravitational source (2.14), and the solution to Eq. (2.16) afforded by Eq. (2.21), the standard approach would represent the inhomogeneous solution to the master equation (2.13) by

$$\Psi_{\ell m}(t, r) \sim \Psi_{\ell m}^{\text{std}}(t, r) = \sum_{n=-N}^{+N} R_{\ell m n}(r) \, e^{-i\omega_{mn}t}, \qquad N \to \infty, \tag{3.3}$$

where we use the $\sim$ to indicate that the equality between the actual solution $\Psi_{\ell m}$ and $\Psi_{\ell m}^{\text{std}}$ holds *almost everywhere* for $N \to \infty$.

Looking ahead somewhat, we use our numerical code to obtain a particular spherical harmonic amplitude, $\Psi_{22}(t, r)$ ($\ell = 2$, $m = 2$), and its radial derivative, $\partial_r \Psi_{22}(t, r)$. We can also use the code to assemble the standard partial Fourier sums (see FIGs. 1 and 2). *We find that the Gibbs problem with the standard approach is significantly worse in the gravitational case (in Regge-Wheeler gauge) than it is for the scalar field.* In the present case the field itself has a discontinuity and the radial derivative is both discontinuous as $r \to r_p(t)$ and also has a delta function singularity at $r_p(t)$. The left panels of FIGs. 1 and 2 are familiar; the partial sums have difficulty representing the jump discontinuity and overshoot the exact solution (solid curve). In the right panels, the singularity at $r_p(t)$ wreaks havoc on the ability of the Fourier synthesis to represent the exact solution.
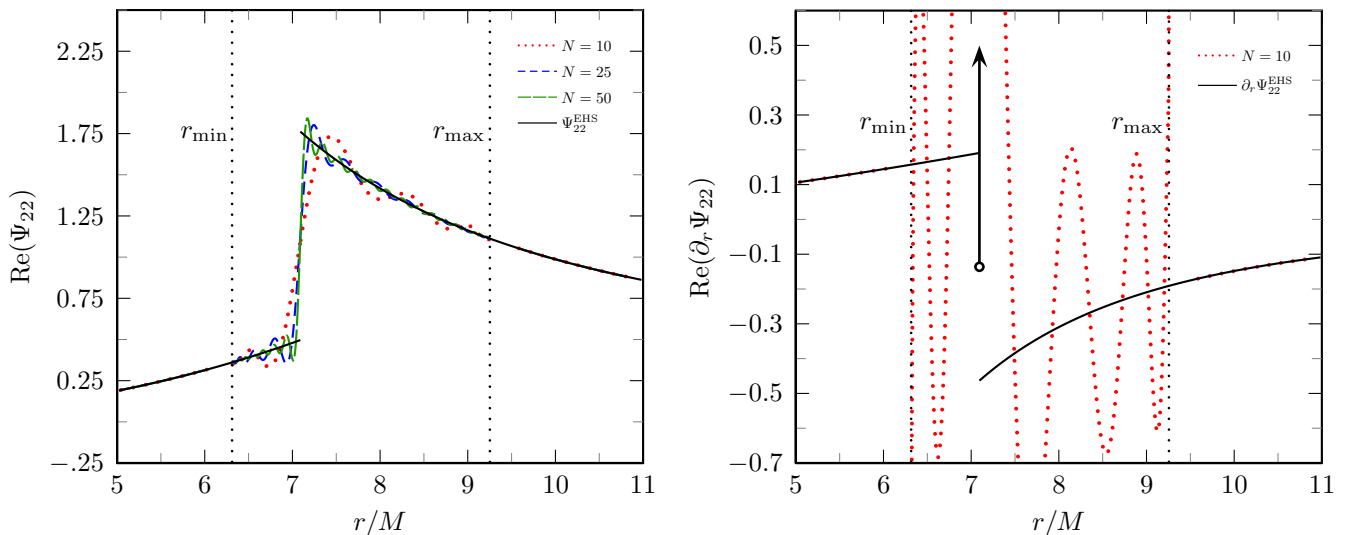

FIG. 1: The standard FD approach to reconstructing the TD master function and its r derivative. The left panel shows Ψ_{22}^{std} and the right shows $\partial_r \Psi_{22}^{\text{std}}$ at $t = 51.78M$ for a particle orbiting with $p = 7.50478$ and $e = 0.188917$. This figure is analogous to FIG. 1 of BOS [38]. Partial sums are computed with Eq. (3.3) and shown for different N. For contrast we plot the converged solution from the new method with a solid curve (see FIG. 3). The arrow in the right panel gives a notional representation of the delta function singularity present in $\partial_r \Psi_{22}$; the amplitude of this singular term is related to the jump in Ψ_{22} seen in the left panel.

On a bright note, outside the range of the source, the standard solution converges exponentially fast. Nevertheless, in the source region between $r_{\min}$ and $r_{\max}$ the convergence will be algebraic in general and disastrous at the location of the particle. A discontinuous (or worse, singular) function cannot be accurately represented by a sum of smooth functions.

We now generalize the EHS method to the gravitational case. We start by recognizing that $R_{\ell m n}^{\pm}$ from Eq. (2.24) are valid solutions to the homogeneous version of Eq. (2.16) throughout the entire domain outside the black hole,

$$R_{\ell m n}^{\pm}(r) = C_{\ell m n}^{\pm} \hat{R}_{\ell m n}^{\pm}(r), \qquad r > 2M. \tag{3.4}$$

Next, we use these to define the *time-domain extended homogeneous solutions*,

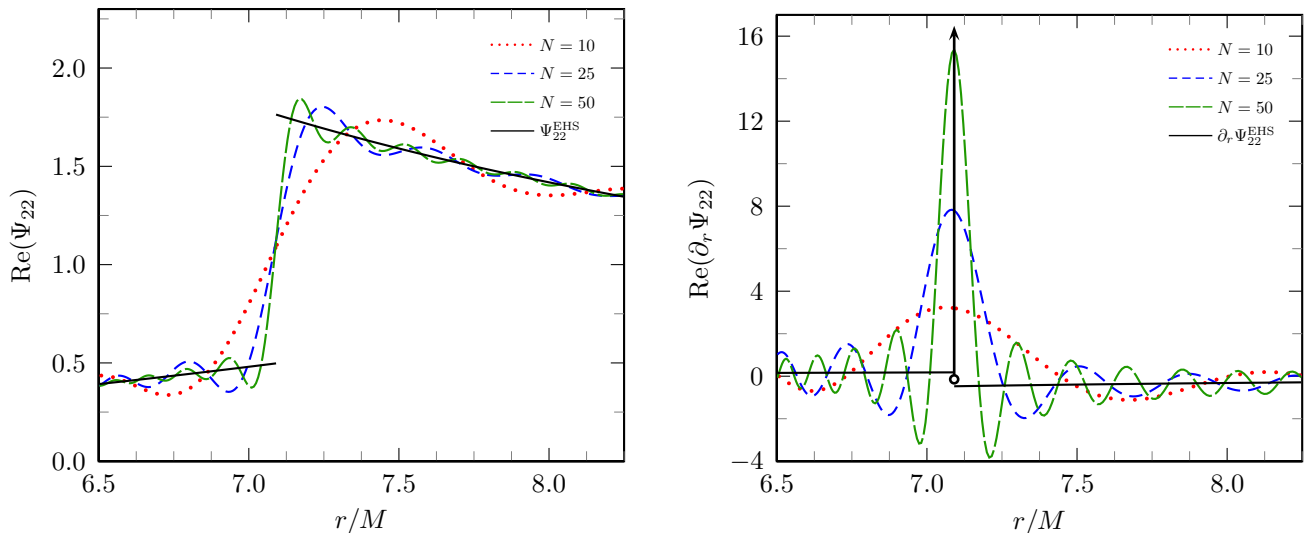$$\Psi_{\ell m}^{\pm}(t, r) \equiv \sum_n R_{\ell m n}^{\pm}(r) \, e^{-i\omega_{mn}t}, \qquad r > 2M, \tag{3.5}$$

FIG. 2: An alternate view of the behavior presented in FIG. 1. A change in the scale in the left panel emphasizes the Gibbs overshoots in Ψ_{22}. On the right, a zoom-out of the vertical scale more clearly indicates the attempt of the Fourier synthesis to capture the delta function at $r_p(t)$.

which result from inserting $R_{\ell mn}^{\pm}$ into Eq. (2.18). The central claim is then that for any t and r the actual solution to the inhomogeneous wave equation (2.13) is given by

$$\Psi_{\ell m}(t,r) = \Psi_{\ell m}^{\mathrm{EHS}}(t,r) \equiv \Psi_{\ell m}^{+}(t,r)\,\theta\left[r - r_p(t)\right] + \Psi_{\ell m}^{-}(t,r)\,\theta\left[r_p(t) - r\right]. \tag{3.6}$$

The argument made by BOS can be extended to the gravitational case and goes as follows:

- We denote the desired true solution of the inhomogeneous wave equation as $\Psi_{\ell m}$. Outside the domain of the source $(r < r_{\min}, r_{\max} < r)$ $\Psi_{\ell m} = \Psi_{\ell m}^{\mathrm{std}} = \Psi_{\ell m}^{\mathrm{EHS}}$ because there $R_{\ell mn} = R_{\ell mn}^{\pm}$.

- It is assumed that $\Psi_{\ell m}(t,r)$ is analytic in the entirety of the two regions $2M < r < r_p(t)$ and $r_p(t) < r$ (excluding only a neighborhood of $r_p(t)$).

- Because the homogeneous solutions $\Psi_{\ell m}^{\pm}$ are expected to be analytic everywhere, $\Psi_{\ell m}^{\mathrm{EHS}}(t,r)$ will be analytic in the two regions discussed above (excluding only a neighborhood of $r_p(t)$). (See the extended discussion BOS have about this.)

- Because $\Psi_{\ell m}$ and $\Psi_{\ell m}^{\mathrm{EHS}}$ are identical outside the region of libration, and they are both analytic everywhere up to the location of the source, they must be equal over that entire domain.

Here we provide an additional justification for the assumed form of the solution given in Eq. (3.6). The source term of the wave equation is a distribution, or generalized function [40]. Accordingly, any solution of Eq. (2.13) will be a weak solution–a generalized function itself–with loss of (classic) differentiability at the singular point $r_p(t)$. To determine the suitability of Eq. (3.6) as a solution of Eq. (2.13), we generalize the concept of differentiation to encompass distributions. Thus, for example, $d\theta(z)/dz = \delta(z)$. We can then take Eq. (3.6) as an ansatz, substitute in Eq. (2.13), and determine what conditions are required that it be a (weak) solution. For clarity, in the rest of this section we suppress the ℓ and m indices.

Rather than use the RWZ equation as it stands, we introduce a coordinate transformation to fix the position of the singularity. Defining $z \equiv r - r_p(t), \bar{t} \equiv t$, the derivatives transform as $\partial_{r_*} = f(r)\partial_z$ and $\partial_t = \partial_{\bar{t}} - \dot{r}_p\partial_z$, and the wave equation (2.13) becomes

$$L(\Psi) = -\partial_{\bar{t}}^2\Psi + \left(f^2 - \dot{r}_p^2\right)\partial_z^2\Psi + 2\dot{r}_p\partial_{\bar{t}}\partial_z\Psi + \left(\ddot{r}_p + (f\partial_z f)\right)\partial_z\Psi - V\Psi = \tilde{G}\,\delta(z) + \tilde{F}\,\delta'(z). \tag{3.7}$$

Now we assume that Ψ has the form given in Eq. (3.6) and substitute it into Eq. (3.7). The functions Ψ^+ and Ψ^- are differentiable and satisfy the homogeneous equation, $L(\Psi^{\pm}) = 0$. A term of the form $L(\Psi^+)\,\theta(z) + L(\Psi^-)\,\theta(-z)$
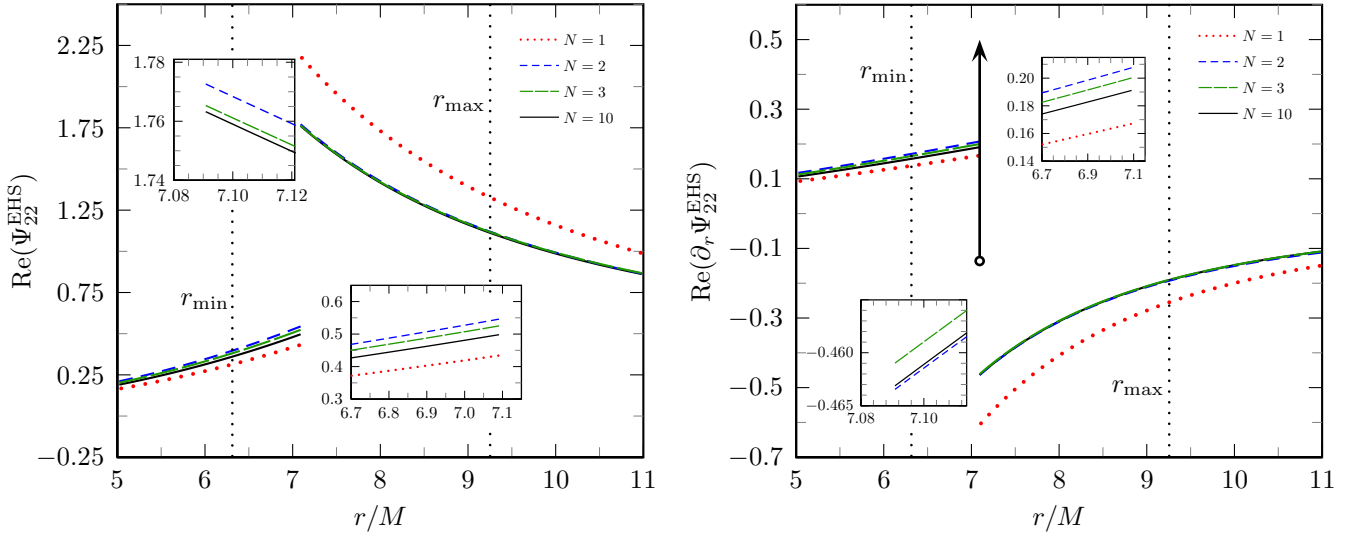
FIG. 3: The EHS approach to reconstructing the TD master function and its radial derivative. As in FIG. 1, we give Ψ_{22}^{EHS} and $\partial_r \Psi_{22}^{\mathrm{EHS}}$ at $t = 51.78M$ for a particle orbiting with $p = 7.50478$ and $e = 0.188917$. Partial sums of Ψ_{22}^{EHS} are computed from Eq. (3.5), with a range of $-N \leq n \leq N$. The full Ψ_{22}^{EHS} and its r derivative result from $N = 10$, which gives agreement in the jumps in Ψ_{22}^{EHS} and $\partial_r \Psi_{22}^{\mathrm{EHS}}$ to a relative error of 10^{-10}. On the right, the presence of a delta function singularity is notionally depicted with an arrow. The time dependent amplitude of this singularity is separately computable from the jump in Ψ_{22}.

appears in (3.7) and drops out. Other singular terms remain, created by derivatives of the Heaviside function, and we are left with

$$\left(f^2 - \dot{r}_p^2\right)\left(\llbracket\partial_r\Psi\rrbracket_p\,\delta(z) + \llbracket\Psi\rrbracket_p\,\delta'(z)\right) + 2\dot{r}_p\partial_{\bar{t}}\left(\llbracket\Psi\rrbracket_p\,\delta(z)\right) + \left(\ddot{r}_p + (f\partial_z f)\right)\llbracket\Psi\rrbracket_p\,\delta(z) = \tilde{G}\,\delta(z) + \tilde{F}\,\delta'(z). \quad (3.8)$$

where

$$\llbracket\Psi\rrbracket_p(t) \equiv \Psi^+\left(t, r_p(t)\right) - \Psi^-\left(t, r_p(t)\right), \qquad \llbracket\partial_r\Psi\rrbracket_p(t) \equiv \partial_r\Psi^+\left(t, r_p(t)\right) - \partial_r\Psi^-\left(t, r_p(t)\right) \quad (3.9)$$

are the jumps in Ψ and $\partial_r\Psi$ at $z = 0$. Naïvely, we might expect that we can simply equate the coefficients of δ on the two sides of Eq. 3.8, while doing the same with the δ' coefficients. However, the δ' term on the left hand side must first be fully evaluated (as a function of time) at the location of the particle. To do this, we use the identities in Eqs. (A1) and (A5), which leaves

$$\left(f_p^2 - \dot{r}_p^2\right)\llbracket\partial_r\Psi\rrbracket_p\,\delta(z) + \left(f_p^2 - \dot{r}_p^2\right)\llbracket\Psi\rrbracket_p\,\delta'(z) - 2\left(f_p\partial_z f_p\right)\llbracket\Psi\rrbracket_p\,\delta(z) + 2\dot{r}_p\partial_{\bar{t}}\left(\llbracket\Psi\rrbracket_p\right)\delta(z)$$
$$+ \left(\ddot{r}_p + (f_p\partial_z f_p)\right)\llbracket\Psi\rrbracket_p\,\delta(z) = \tilde{G}\,\delta(z) + \tilde{F}\,\delta'(z), \quad (3.10)$$

where $f_p \equiv f(r_p(t))$. Note that there is no comparable expansion on the right side from the $\tilde{F}\,\delta'(z)$ term because $\tilde{F}$ is already fully evaluated at $r = r_p(t)$, by design. From here, we read off the jumps in Ψ and its r derivative at $r_p(t)$ from the coefficients of δ' and δ, respectively. Returning to Schwarzschild coordinates and using Eqs. (2.12) to remove $\ddot{r}_p$ and $\dot{r}_p^2$ terms, we find

$$\llbracket\Psi\rrbracket_p(t) = \frac{\mathcal{E}^2}{f_p^2 U_p^2}\tilde{F}(t), \qquad \llbracket\partial_r\Psi\rrbracket_p(t) = \frac{\mathcal{E}^2}{f_p^2 U_p^2}\left[\tilde{G}(t) + \frac{1}{U_p^2 r_p^2}\left(3M - \frac{\mathcal{L}^2}{r_p} + \frac{5M\mathcal{L}^2}{r_p^2}\right)\tilde{F}(t) - 2\dot{r}_p\frac{d}{dt}\left(\llbracket\Psi\rrbracket_p\right)\right]. \quad (3.11)$$

From the standpoint of the original coordinates, the partial time derivative $\partial_{\bar{t}}$ becomes the convective, or total, time derivative along the particle worldline.

These jump conditions amount to internal boundary conditions that are necessary conditions on a solution to the inhomogeneous wave equation in the TD. They were discussed by Sopuerta and Laguna [35] and also later, with corrections, by Field et al. [44]. In our FD-based calculations, they provide a powerful check on our transformation of the solutions back to the TD. Given the indirect way in which the Fourier transform of the source $S_{\ell m}$ determines the Fourier coefficients of the extended homogeneous solutions, considerable credence is lent to the method in seeing

the partial sums of $\Psi_{\ell m}^{\text{EHS}}$ converge toward satisfying these jump conditions. Secondarily, the jump conditions provide useful stopping criteria in the numerical method (see Sec. IV C).

While not a focus of this paper, we consider briefly TD simulations. There, to find a unique solution the internal boundary conditions must be augmented with initial data on a Cauchy surface and, potentially, outer boundary conditions. Care must be exercised to switch on the source smoothly in the (near) future of the initial value surface [44] (also Lau, private communication). Additionally, imposed initial data will not typically match long term periodic behavior induced by the source, and transients will sweep through the system for several dynamical times. In contrast, in the FD approach, the proper outgoing and downgoing behavior at the outer boundaries is built in from the outset and only the steady state, periodic behavior is obtained.

C. Computing normalization coefficients in the gravitational case

Finally, we provide some details on how the singular source is integrated to provide the matching normalization coefficients $C_{\ell mn}^{+}$ and $C_{\ell mn}^{-}$ that are used in Eq. (3.4). BOS detail the calculation of normalization coefficients for the scalar monopole in their App. C. The gravitational case follows the same general idea, but involves some technical differences and challenges. We start by combining Eqs. (2.25) and (2.22), giving

$$C_{\ell mn}^{\pm} = \frac{1}{W_{\ell mn}} \int_{r_{\min}}^{r_{\max}} dr \, \frac{\hat{R}_{\ell mn}^{\mp}(r) Z_{\ell mn}(r)}{f(r)}. \tag{3.12}$$

The FD source term $Z_{\ell mn}(r)$ comes from plugging Eq. (2.14) into Eq. (2.17), yielding

$$Z_{\ell mn}(r) = \frac{1}{T_r} \int_0^{T_r} dt \, \left(\tilde{G}_{\ell m}(t) \, \delta[r - r_p(t)] + \tilde{F}_{\ell m}(t) \, \delta'[r - r_p(t)] \right) e^{i\omega_{mn}t}. \tag{3.13}$$

The equivalent integral BOS present for the scalar monopole is their Eq. (C2), which they evaluate immediately by changing the integration variable from t to r_p. Here, with a derivative-of-the-delta function present (in RWZ gauge), the immediate evaluation of this integral produces terms that are singular at the turning points ($\dot{r}_p = 0$). These terms are no problem analytically, but they are troublesome when performing the final numerical integration. We therefore find it is advantageous to delay this integration. Plugging our expression for $Z_{\ell mn}$ in above, we have

$$C_{\ell mn}^{\pm} = \frac{1}{W_{\ell mn} T_r} \int_{r_{\min}}^{r_{\max}} dr \, \frac{\hat{R}_{\ell mn}^{\mp}(r)}{f(r)} \int_0^{T_r} dt \, \left(\tilde{G}_{\ell m}(t) \, \delta[r - r_p(t)] + \tilde{F}_{\ell m}(t) \, \delta'[r - r_p(t)] \right) e^{i\omega_{mn}t}. \tag{3.14}$$

In order to avoid the singularity at the turning points, we switch the order of integration. The integration of the delta function itself is then straightforward. The derivative of δ term requires an integration by parts. Because of the compact support of the source term, we can extend the range of integration and no surface terms appear. We are left with

$$C_{\ell mn}^{\pm} = \frac{1}{W_{\ell mn} T_r} \int_0^{T_r} \left[\frac{1}{f_p} \hat{R}_{\ell mn}^{\mp}(r_p) \tilde{G}_{\ell m}(t) + \left(\frac{2M}{r_p^2 f_p^2} \hat{R}_{\ell mn}^{\mp}(r_p) - \frac{1}{f_p} \frac{d\hat{R}_{\ell mn}^{\mp}(r_p)}{dr} \right) \tilde{F}_{\ell m}(t) \right] e^{i\omega_{mn}t} \, dt, \tag{3.15}$$

where we use a p subscript to indicate evaluation of a quantity at $r = r_p(t)$. Our final integral is analogous to Eq. (C7) in BOS.

Here is a summary of key details of the application of the method in the gravitational case:

- The EHS method, applied to the gravitational case, gives exponentially converging solutions to Eq. (2.13) everywhere, including the location of the particle. (See FIG. 4.)

- Working in Regge-Wheeler gauge, the gravitational TD source term contains a delta function and a derivative-of-the-delta function, which cause $\Psi_{\ell m}$ to exhibit a jump and $\partial_r \Psi_{\ell m}$ to exhibit both a jump and a delta function singularity at the particle's location. (See FIG. 3.) In the scalar case, the field is piecewise continuous at the particle, with a jump in the r derivative. (See FIG. 3 in BOS.)

- Eq. (3.15) is valid for all radiative multipoles ($\ell \geq 2$). The $\ell = 0, 1$, modes must be handled separately.

- Martel's [30] $G_{\ell m}(t, r)$ and $F_{\ell m}(t, r)$ from Eq. (1.1) are not in fully evaluated form. As discussed in App. A, for a given multipole, unique functions of time $\tilde{F}_{\ell m}(t) \equiv F_{\ell m}(t, r_p(t))$ and $\tilde{G}_{\ell m}(t) \equiv G_{\ell m}(t, r_p(t)) - \partial_r F_{\ell m}(t, r_p(t))$ emerge after fully applying the delta function constraint. We use the tilde to distinguish fully evaluated coefficients.

- In practice, we take advantage of the fact that some of the functions in the integrand of Eq. (3.15) are even over the period of radial libration, while others are odd. Then, rather than integrating over t from $0 \to T_r$, we can limit the range of integration to $0 \to T_r/2$. Further, we change variables to χ, as shown in Sec. II A and integrate from $0 \to \pi$.

- For $\Psi_{\ell m}^{\text{even}}$ we use the Zerilli-Moncrief master function, and for $\Psi_{\ell m}^{\text{odd}}$ we use the Cunningham-Price-Moncrief master function. This formulation works for any master function that obeys a Regge-Wheeler-like equation and has a source term that can be written in the form of Eq. (2.14).

IV. NUMERICAL METHOD AND RESULTS FROM MODE INTEGRATIONS

A. Algorithmic roadmap

Here, we explain the specific steps our code takes to solve the inhomogeneous wave equation (2.13). There are several stages to the process, and at each step we compute at least one more order of magnitude accuracy than is needed at the subsequent step. The code is written in C, and we use the Numerical Recipes adaptive step size fourth order Runge-Kutta integrator [48].

1. Specify an orbit through a choice of the semi-latus rectum p and eccentricity e.

2. Numerically integrate Eqs. (2.10) and (2.11) to get the fundamental frequencies of the system, Ω_r and Ω_φ, and hence $\omega_{mn} = m\Omega_\varphi + n\Omega_r$.

3. Choose a specific ℓ and m. If $\ell + m$ is even (odd), use even (odd) parity potential and source terms. Choose starting n. (See Sec. IV C.)

4. Solve the homogeneous version of Eq. (2.16) to get unit normalized radial mode functions, $\hat{R}_{\ell mn}^{\pm}$, in the source-free region:

   - Use the asymptotic expansion (see App. D) to set an "up" plane wave boundary condition at $r_* \to +\infty$, as in Eq. (2.20). Numerically integrate up to the region of the source at r_*^{max} to get $\hat{R}_{\ell mn}^{+}$. (We let $r_*^{\text{min/max}}$ be the r_* value corresponding to $r_{\text{min/max}}$.)
   - Use a convergent Taylor expansion to set an "in" plane wave boundary condition (Eq. (2.19)) at modestly negative r_*. Numerically integrate up to the region of the source at r_*^{min} to get $\hat{R}_{\ell mn}^{-}$.

5. Solve the homogeneous version of Eq. (2.16) to continue the unit normalized radial mode functions, $\hat{R}_{\ell mn}^{\pm}$, into the source region, while also computing the normalization coefficients $C_{\ell mn}^{\pm}$:

   - Simultaneously integrate Eqs. (2.16) and (3.15) from $\chi = 0 \to \pi$ (equivalently $t = 0 \to T_r/2$ and $r = r_{\text{min}} \to r_{\text{max}}$). This gives $\hat{R}_{\ell mn}^{-}$ in the region of the source and $C_{\ell mn}^{+}$.
   - Simultaneously integrate Eqs. (2.16) and (3.15) from $\chi = -\pi \to 0$ (equivalently $t = -T_r/2 \to 0$ and $r = r_{\text{max}} \to r_{\text{min}}$). This gives $\hat{R}_{\ell mn}^{-}$ in the region of the source and $C_{\ell mn}^{-}$.

   As discussed in Sec. III C, the integrand in Eq. (3.15) contains parts which are even and parts which are odd over the radial period. By keeping the correct terms, we can get away with efficiently integrating over only half the period.

6. Use the coefficients to normalize the homogeneous solutions outside *and inside* the range of the source, as in Eq. (3.4).

7. Assess whether there is convergence of the partial sum over n. (Again, see Sec. IV C.)

   - If yes, we are finished with this ℓ, m mode.
   - If no, return to Step 4 with the next n.

B. Energy and angular momentum fluxes at $r_* = \pm\infty$

To evaluate the energy and angular momentum fluxes at $r_* = \pm\infty$ we use the Isaacson stress-energy tensor. The energy and angular momentum fluxes, for each ℓ, m mode, can be written as [49]

$$\dot{E}^{\pm}_{\ell m} = \frac{1}{64\pi} \frac{(\ell+2)!}{(\ell-2)!} \left| \dot{\Psi}^{\pm}_{\ell m}(t,r) \right|^2, \qquad \dot{L}^{\pm}_{\ell m} = \frac{im}{64\pi} \frac{(\ell+2)!}{(\ell-2)!} \dot{\Psi}^{\pm}_{\ell m}(t,r) \Psi^{\pm *}_{\ell m}(t,r). \tag{4.1}$$

Here, an asterisk signifies complex conjugation. (We use $\Psi^{\mathrm{even}}_{\ell m}$ when $\ell + m$ is even and $\Psi^{\mathrm{odd}}_{\ell m}$ when $\ell + m$ is odd. In general there would be contributions from both $\Psi^{\mathrm{even}}_{\ell m}$ and $\Psi^{\mathrm{odd}}_{\ell m}$ for each mode, but our choice of $\theta_p = \pi/2$ leads to one of these functions vanishing for each ℓ and m combination.) In terms of FD amplitudes the expressions become

$$\dot{E}^{\pm}_{\ell m} = \frac{1}{64\pi} \frac{(\ell+2)!}{(\ell-2)!} \sum_{n,n'} \omega_{mn} \omega_{mn'} R^{\pm}_{\ell mn} R^{\pm *}_{\ell mn'} e^{-i(\omega_{mn} - \omega_{mn'})t},$$

$$\dot{L}^{\pm}_{\ell m} = \frac{m}{64\pi} \frac{(\ell+2)!}{(\ell-2)!} \sum_{n,n'} \omega_{mn} R^{\pm}_{\ell mn} R^{\pm *}_{\ell mn'} e^{-i(\omega_{mn} - \omega_{mn'})t}. \tag{4.2}$$

As is well known, the fluxes must be suitably averaged over time or space to obtain meaningful, invariant results. We average these quantities in time over one radial oscillation, which yields

$$\left\langle \dot{E}^{\pm}_{\ell m} \right\rangle = \frac{1}{64\pi} \frac{(\ell+2)!}{(\ell-2)!} \sum_n \omega^2_{mn} \left| C^{\pm}_{\ell mn} \hat{R}^{\pm}_{\ell mn} \right|^2, \qquad \left\langle \dot{L}^{\pm}_{\ell m} \right\rangle = \frac{m}{64\pi} \frac{(\ell+2)!}{(\ell-2)!} \sum_n \omega_{mn} \left| C^{\pm}_{\ell mn} \hat{R}^{\pm}_{\ell mn} \right|^2. \tag{4.3}$$

Here, we have also introduced $R^{\pm}_{\ell mn} = C^{\pm}_{\ell mn} \hat{R}^{\pm}_{\ell mn}$. As discussed in App. D, we can write the radial function as $\hat{R}^{\pm}_{\ell mn}(r) = J^{\pm}_{\ell mn}(r) e^{\pm i\omega_{mn} r_*}$, where $J^{\pm}_{\ell mn}(r) \to 1$ as $r_* \to \pm\infty$. Therefore, if we set $J^{\pm}_{\ell mn} = 1$, we can evaluate the fluxes at $r_* = \pm\infty$, leaving

$$\left\langle \dot{E}^{\pm\infty}_{\ell m} \right\rangle = \frac{1}{64\pi} \frac{(\ell+2)!}{(\ell-2)!} \sum_n \omega^2_{mn} \left| C^{\pm}_{\ell mn} \right|^2, \qquad \left\langle \dot{L}^{\pm\infty}_{\ell m} \right\rangle = \frac{m}{64\pi} \frac{(\ell+2)!}{(\ell-2)!} \sum_n \omega_{mn} \left| C^{\pm}_{\ell mn} \right|^2. \tag{4.4}$$

C. Code validation

To compute the total energy and angular momentum fluxes, we must sum Eqs. (4.4) over ℓ and m. The resulting expressions are formally over the ranges $2 \le \ell \le \infty$, $-\ell \le m \le \ell$, $-\infty \le n \le \infty$. When computing $\dot{E}$ and $\dot{L}$ numerically, we put limits on each of these sums. To begin with, the low ℓ modes matter more than the high ones. But, the more eccentric an orbit, the more ℓ's must be computed to achieve the same precision in our final values. For the orbits we considered in Table I, in order to achieve a relative precision of 10^{-12} in our final flux values, the highest ℓ necessary was $\ell = 29$. (See Sec. IV D.)

Because of the symmetry of the spherical harmonics, the fluxes from any given $-m$ mode are equal to those from the corresponding $+m$ mode. Therefore, we fold the negative m modes over onto the positive ones, and simply multiply each positive m mode by two. Additionally, as ℓ gets larger, it is no longer necessary to compute all m values. As can be seen in Table III, for a given ℓ, the largest $\dot{E}^{\infty/H}_{\ell m}$ and $\dot{L}^{\infty/H}_{\ell m}$ contributions come from the $m = \ell$ mode. We start at $m = \ell$ and decrement m until the fluxes are no longer significant. For low ℓ values we still wind up computing all $0 \le m \le \ell$, but as ℓ increases, we need progressively fewer m modes.

Determining the necessary n's is a bit more involved. For a given ℓ and m, there is a range, n_{min} to n_{max}, over which we sum in order to achieve our desired precision. Looking at Table III, it is evident that when $m = 0$, the range of n is essentially centered on 0. For these modes, we start with $n = 0$, and compute fluxes for all positive modes. When we have seen no change to any of the flux values (at a pre-specified level of precision) for several consecutive modes, we stop and repeat the process for the negative n's. As m increases, this range of n's shifts more and more into the positive. For any ℓ, the $m = \ell$ mode has far more positive n modes than negative. Eventually, ℓ becomes so large that $n_{\mathrm{min}} > 0$ for the $m = \ell$ mode. For modes where we suspect that $n_{\mathrm{min}} > 0$, we find it advantageous to start with a rough sweep of a large range of possible n values. We calculate $\dot{E}^{\infty}_{\ell mn}$ (the energy flux at $r = +\infty$ from one n mode) to low precision for a small number of n, spaced out over this range. The n for which we find the largest $\dot{E}_{\ell mn}$ will be near the center of the n_{min} to n_{max} range. We then perform our high precision mode integrations for all significant n values above and below this n.

If we are interested in a local calculation (as one would perform for a SF evaluation), we have a different method for determining which n's are significant. We still use the energy fluxes to find the approximate center of the significant n range, but for the "breaking condition" we compute n's until the jumps in $\Psi_{\ell m}$ and $\partial_r \Psi_{\ell m}$ converge properly, as follows:

- Use Eq. (3.5) to compute a partial mode sum approximation of both $\Psi_{\ell m}^{\pm}(t, r_p)$ and $\partial_r \Psi_{\ell m}^{\pm}(t, r_p)$ for a large number of times t_k throughout the orbit.

- Numerically evaluate the jumps in those partial sums

$$\left[\!\left[\Psi_{\ell m}^N\right]\!\right]_p \equiv \Psi_{\ell m}^+ (t, r_p) - \Psi_{\ell m}^- (t, r_p), \qquad \left[\!\left[\partial_r \Psi_{\ell m}^N\right]\!\right]_p \equiv \partial_r \Psi_{\ell m}^+ (t, r_p) - \partial_r \Psi_{\ell m}^- (t, r_p), \qquad (4.5)$$

for those times t_k.

- Compute the analytical values of $\left[\!\left[\Psi_{\ell m}^A\right]\!\right]_p$ and $\left[\!\left[\partial_r \Psi_{\ell m}^A\right]\!\right]_p$ derived in Sec. III B for those times t_k.

- If $\left[\!\left[\Psi_{\ell m}^N\right]\!\right]_p = \left[\!\left[\Psi_{\ell m}^A\right]\!\right]_p$ and $\left[\!\left[\partial_r \Psi_{\ell m}^N\right]\!\right]_p = \left[\!\left[\partial_r \Psi_{\ell m}^A\right]\!\right]_p$ at all times t_k, to a chosen precision, we have computed enough n modes.

- Otherwise more n modes are needed. As in the flux computation case above, we perform the mode calculations for the n values above our starting n, and once that partial sum has converged to our desired precision, we solve for the n's below our starting n until the jump values agree.

D. Results

One of our most important results is the exponential convergence of $\Psi_{\ell m}^{\mathrm{EHS}}$ and its r derivative at the location of the particle. FIG. 3 shows a partial sum of these two quantities converging after only a few modes. Compare this to FIGs. 1 and 2, which shows the standard FD approach. In particular, note in those figures the failure of the standard approach to accurately represent $\partial_r \Psi_{\ell m}$, even after a large number of modes. This function is particularly badly behaved in the standard approach as smooth functions attempt to capture a delta function.

Also of note is FIG. 4, which shows that the convergence from the method of extended homogeneous solutions is indeed exponential, all the way up to the location of the particle. Fast and accurate computation of $\Psi_{\ell m}$ and $\partial_r \Psi_{\ell m}$ at $r_p(t)$ will eventually be critical for reliable local SF calculations.
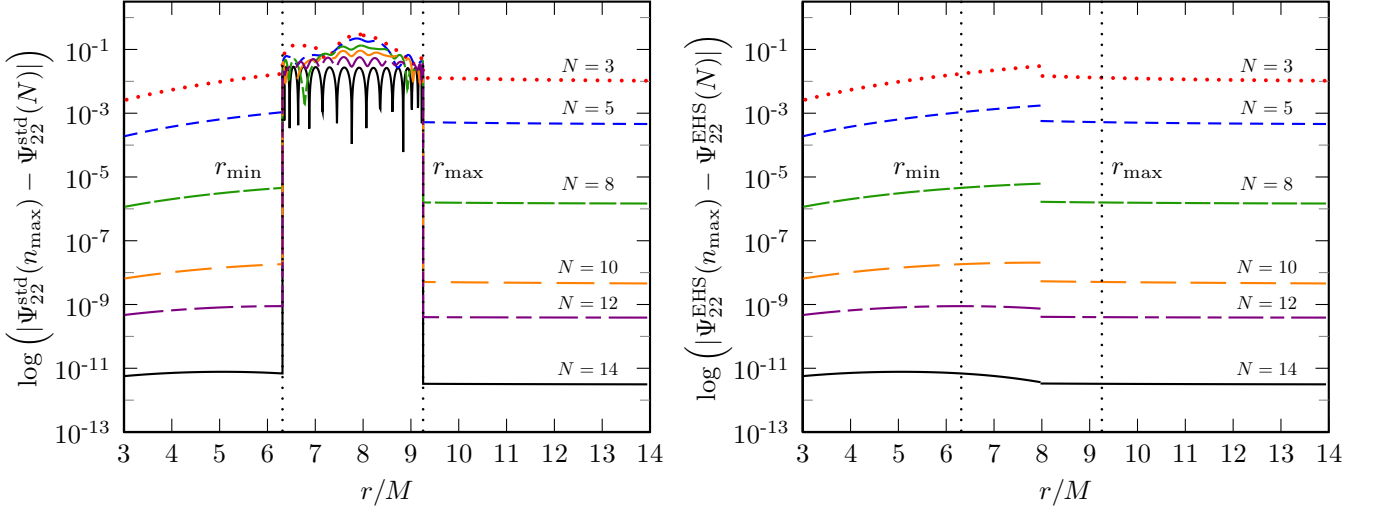

FIG. 4: A plot of the convergence of the master function using the two methods. For a particle orbiting with $p = 7.50478$ and $e = 0.188917$ at $t = 51.78M$ we compute the master function $\Psi_{22}(n_{\max})$ by summing over modes ranging from $-n_{\max} \leq n \leq n_{\max}$ for $n_{\max} = 15$. We plot the log of the difference between $\Psi_{22}(n_{\max})$ and the partial sum $\Psi_{22}(N)$, for different $N < n_{\max}$. For the standard approach (left), we see exponential convergence in the homogeneous region, but only algebraic convergence in the region of the source. The method of extended homogeneous solutions (right) yields exponentially converging results at all points outside *and inside* the region of the source. The method of extended homogeneous solutions gives exponential convergence for $\partial_r \Psi_{\ell m}^{\mathrm{EHS}}$ as well.

	$\dot{E}^{\infty}_{\ell m}$ (M^2/μ^2)	$\dot{E}^{H}_{\ell m}$ (M^2/μ^2)	$\dot{L}^{\infty}_{\ell m}$ (M/μ^2)	$\dot{L}^{H}_{\ell m}$ (M/μ^2)
$p = 7.50478,\ e = 0.188917$				
This Paper, $\ell_{\max} = 23$	$3.16899989185 \times 10^{-4}$	$5.23247295625 \times 10^{-7}$	$5.96755215609 \times 10^{-3}$	$8.71943028067 \times 10^{-6}$
Fujita et al.	$3.16899989184 \times 10^{-4}$	N/A	$5.96755215608 \times 10^{-3}$	N/A
$p = 8.75455,\ e = 0.764124$				
This Paper, $\ell_{\max} = 29$	$2.12360313360 \times 10^{-4}$	$2.27177440621 \times 10^{-6}$	$2.77735939025 \times 10^{-3}$	$2.22781961809 \times 10^{-5}$
Fujita et al.	$2.12360313326 \times 10^{-4}$	N/A	$2.77735938996 \times 10^{-3}$	N/A

TABLE I: Total energy and angular momentum fluxes for eccentric orbits, compared with those from Fujita et al., published in [14].

	$\dot{E}^{\infty}_{\ell m}$ (M^2/μ^2)	$\dot{E}^{H}_{\ell m}$ (M^2/μ^2)	$\dot{L}^{\infty}_{\ell m}$ (M/μ^2)	$\dot{L}^{H}_{\ell m}$ (M/μ^2)
$p = 10,\ e = 0.1$				
This Paper	$6.31752474718 \times 10^{-5}$	$1.53365819446 \times 10^{-8}$	$1.95274165241 \times 10^{-3}$	$4.48832141611 \times 10^{-7}$
Fujita et al.	$6.31752474720 \times 10^{-5}$	$1.53365819445 \times 10^{-8}$	N/A	N/A
$p = 10,\ e = 0.5$				
This Paper	$9.27335011599 \times 10^{-5}$	$1.41298859263 \times 10^{-7}$	$1.97465149446 \times 10^{-3}$	$2.15617302381 \times 10^{-6}$
Fujita et al.	$9.27335011503 \times 10^{-5}$	$1.41298859260 \times 10^{-7}$	N/A	N/A
$p = 10,\ e = 0.7$				
This Paper	$9.46979134556 \times 10^{-5}$	$3.55415030147 \times 10^{-7}$	$1.63064691133 \times 10^{-3}$	$4.20771917244 \times 10^{-6}$
Fujita et al.	$9.46979134409 \times 10^{-5}$	$3.55415030114 \times 10^{-7}$	N/A	N/A
$p = 10,\ e = 0.9$				
This Paper	$4.194264692 \times 10^{-5}$	$3.652142848 \times 10^{-7}$	$5.982866119 \times 10^{-3}$	$3.518978461 \times 10^{-6}$
Fujita et al.	$4.19426469206 \times 10^{-5}$	$3.65214284306 \times 10^{-7}$	N/A	N/A

TABLE II: Energy and angular momentum fluxes for eccentric orbits, compared with those from Fujita et al. [51]. Partial sums for all four orbits are truncated at $\ell_{\max} = 20$ for both papers. Fujita et al. obtained their numbers from integrating the Teukolsky equation. We include this table to show the agreement of our horizon energy flux values.

In order to check our code's accuracy, we computed energy and angular momentum fluxes for circular and eccentric orbits. Our circular orbit fluxes agree, mode-by-mode, with published results (e.g. Cutler et al. [50]) to high precision. For eccentric orbits, we are only aware that total energy and angular momentum fluxes have been published. Our FD results agree with the fluxes at $r \to \infty$ of Fujita et al., published in [14] to at least 10^{-9}. These are included in Table I. Fujita et al. have also published horizon energy fluxes [51], which we agree with, to at least 10^{-9} for a range of eccentricities. These are given in Table II.

For those wishing to reproduce our results, in Table III we give mode-by-mode fluxes up to $\ell = 5$ at $r = \infty$ and down the black hole at $r = 2M$ for a particle in orbit with $p = 8.75455$ and $e = 0.764124$. Included are the ranges of n modes summed over to achieve these results.

As expected, our code is more efficient for low eccentricities. The first orbit in Table I ($p = 7.50478$, $e = 0.188917$), runs in under a half hour on a single processor machine, giving the total flux for all $2 \le \ell \le 23$ (although note the limits on m and n mentioned in the previous subsection) to a fractional error of 10^{-12}. As e increase, though, run times increase greatly. The second orbit in that table ($p = 8.75455$, $e = 0.764124$) takes six hours to achieve the same accuracy for all necessary $2 \le \ell \le 29$. And, when $e = 0.9$ for $2 \le \ell \le 20$ in the last row of Table II, we had to raise our fractional error to 10^{-10} in order to get a run time of eighteen hours.

Clearly, as e gets close to 1, FD methods will lose out to TD codes, which handle high eccentricities with more ease. Still for $0 \le e \lesssim 0.9$, our run times are not unreasonable when considering the high accuracy we achieve.

V. RECONSTRUCTION OF THE METRIC PERTURBATION AMPLITUDES

The full benefit of having complete and highly converged solutions for the master functions lies in using them to reconstruct the metric. Ultimately, one wants to use the information, along with an appropriate regularization scheme, to compute the self force. A developed approach to doing this is the mode-sum regularization method [52], which makes use of Lorenz gauge. Here we use the information encoded in the master functions to compute accurately

ℓ	m	$\dot{E}^\infty_{\ell m}$ (M^2/μ^2)	$\dot{E}^H_{\ell m}$ (M^2/μ^2)	$\dot{L}^\infty_{\ell m}$ (M/μ^2)	$\dot{L}^H_{\ell m}$ (M/μ^2)	$n_{\min}$	$n_{\max}$
2	0	$1.27486196317 \times 10^{-8}$	$1.66171571270 \times 10^{-8}$	0	0	-74	76
	1	$1.15338054092 \times 10^{-6}$	$3.08063328605 \times 10^{-7}$	$1.44066000650 \times 10^{-5}$	$2.77518962557 \times 10^{-6}$	-62	78
	2	$1.55967717209 \times 10^{-4}$	$1.84497995136 \times 10^{-6}$	$2.07778922470 \times 10^{-3}$	$1.85014840343 \times 10^{-5}$	-47	82
3	0	$2.53527063853 \times 10^{-11}$	$1.23159713946 \times 10^{-10}$	0	0	-84	85
	1	$9.66848921204 \times 10^{-10}$	$2.47099909183 \times 10^{-9}$	$1.93528074730 \times 10^{-8}$	$2.10622579957 \times 10^{-8}$	-66	87
	2	$6.17859627641 \times 10^{-7}$	$1.29412677182 \times 10^{-8}$	$7.54192378736 \times 10^{-6}$	$1.23105502765 \times 10^{-7}$	-48	93
	3	$3.71507683858 \times 10^{-5}$	$8.07017762262 \times 10^{-8}$	$4.67102471030 \times 10^{-4}$	$7.99808068724 \times 10^{-7}$	-34	99
4	0	$1.14820411420 \times 10^{-12}$	$1.50591364139 \times 10^{-12}$	0	0	-80	80
	1	$4.58377338924 \times 10^{-12}$	$2.04365875527 \times 10^{-11}$	$4.50183584238 \times 10^{-11}$	$1.63314060565 \times 10^{-10}$	-77	94
	2	$1.59253324588 \times 10^{-9}$	$1.62313574547 \times 10^{-10}$	$2.40079049220 \times 10^{-8}$	$1.51029853345 \times 10^{-9}$	-51	93
	3	$2.44084848389 \times 10^{-7}$	$6.50157912447 \times 10^{-10}$	$2.91633622588 \times 10^{-6}$	$6.23354901544 \times 10^{-9}$	-34	106
	4	$1.12530626433 \times 10^{-5}$	$4.66621235553 \times 10^{-9}$	$1.37037638198 \times 10^{-4}$	$4.59633939401 \times 10^{-8}$	-31	114
5	0	$2.93546198223 \times 10^{-15}$	$1.68762144246 \times 10^{-14}$	0	0	-94	94
	1	$1.66341467681 \times 10^{-13}$	$2.73842758121 \times 10^{-13}$	$1.99357707469 \times 10^{-12}$	$2.10992243393 \times 10^{-12}$	-77	92
	2	$1.72172010497 \times 10^{-12}$	$1.49178217605 \times 10^{-12}$	$2.59625132235 \times 10^{-11}$	$1.34307539131 \times 10^{-11}$	-63	100
	3	$1.73935003471 \times 10^{-9}$	$1.01021973779 \times 10^{-11}$	$2.26258058740 \times 10^{-8}$	$9.56603438989 \times 10^{-11}$	-46	109
	4	$9.01787571564 \times 10^{-8}$	$3.64807139949 \times 10^{-11}$	$1.06079902733 \times 10^{-6}$	$3.50623060712 \times 10^{-10}$	-29	121
	5	$3.74854353561 \times 10^{-6}$	$3.02291684853 \times 10^{-10}$	$4.47051998131 \times 10^{-5}$	$2.96568439531 \times 10^{-9}$	-19	130
Total		$2.10242675876 \times 10^{-4}$	$2.27174892328 \times 10^{-6}$	$2.75262625234 \times 10^{-3}$	$2.22779475534 \times 10^{-5}$		

TABLE III: Energy and angular momentum fluxes for an eccentric orbit with $p = 8.75455$, $e = 0.764124$. Note that we have folded the negative m modes onto the corresponding positive m modes and doubled the flux values in this table for $m > 0$.

the spherical harmonic amplitudes of the metric perturbation in Regge-Wheeler gauge. The ability to determine the metric at all locations, including at the particle location, should serve as a useful starting point for computing the SF, either via a gauge transformation or an alternative regularization technique.

We summarize the metric perturbation (MP) formalism in App. C, where the definitions of the master functions, $\Psi^{\text{even}}_{\ell m}$ and $\Psi^{\text{odd}}_{\ell m}$, are given in terms of spherical harmonic amplitudes of the metric and their radial derivatives. We reserve for this section giving the equations, (5.5) and (5.15), for reconstructing the metric amplitudes in Regge-Wheeler gauge from the master functions. These equations involve first derivatives, and in some cases second derivatives, of the master functions. They also involve spherical harmonic projections of the stress-energy tensor. Based on the form (1.2) anticipated in a master function, both of the abovementioned facts contribute to an expectation that the MP amplitudes might have point-singular behavior at $r_p(t)$ in the form of both δ and δ' terms. We show that all potential δ' terms cancel out. However, in general a MP amplitude might have a functional form

$$M(t,r) = M^+(t,r)\,\theta(z) + M^-(t,r)\,\theta(-z) + M^S(t)\,\delta(z), \qquad z \equiv r - r_p(t), \tag{5.1}$$

where M^+ (M^-) represents a smooth function in the region $r > r_p$ ($r < r_p$), and M^S is a smooth function of t alone, giving the magnitude of the singularity. We examine M^S for all six non-zero MP amplitudes in the Regge-Wheeler gauge, and find three such terms to be nonvanishing. Throughout the rest of this section we again suppress spherical harmonic labels ℓ and m.

As mentioned the metric reconstruction equations, of each parity, require spherical harmonic projections of the stress-energy tensor. For a particle of mass μ, traveling on a geodesic of the background spacetime, with four-velocity u^μ, it is

$$T^{\mu\nu}(x^\alpha) = \mu \int \frac{d\tau}{\sqrt{-g}} u^\mu(\tau) u^\nu(\tau)\, \delta^4\left[x - x_p(\tau)\right]. \tag{5.2}$$

In Schwarzschild coordinates the determinant of the metric is $g = -r^4 \sin^2\theta$. After changing the variable of integration to coordinate time t, we have

$$T^{\mu\nu}(x^\alpha) = \frac{\mu\, u^\mu(t) u^\nu(t)}{u^t(t)\, r_p(t)^2}\, \delta[r - r_p(t)]\, \delta[\varphi - \varphi_p(t)]\, \delta[\theta - \pi/2]. \tag{5.3}$$

Spherical harmonic projections of $T^{\mu\nu}$ appear as source terms in the decomposed Einstein equations (App. C) and these are in turn combined to produce the source terms for the master equations (App. B). In the subsections that

follow, we evaluate the time dependence of all of the stress-energy tensor projections. We use the definitions

$$\Lambda(r) \equiv \lambda + \frac{3M}{r}, \qquad \lambda \equiv \frac{(\ell+2)(\ell-1)}{2}. \tag{5.4}$$

A. Even parity

The even parity MP amplitudes are expressed in terms of Ψ_{even} and the source terms by (see [30])

$$K(t,r) = f\partial_r \Psi_{\text{even}} + A\,\Psi_{\text{even}} - \frac{r^2 f^2}{(\lambda+1)\Lambda} Q^{tt},$$

$$h_{rr}(t,r) = \frac{\Lambda}{f^2}\left[\frac{\lambda+1}{r}\Psi_{\text{even}} - K\right] + \frac{r}{f}\partial_r K, \tag{5.5}$$

$$h_{tr}(t,r) = r\partial_t\partial_r\Psi_{\text{even}} + rB\,\partial_t\Psi_{\text{even}} - \frac{r^2}{\lambda+1}\left[Q^{tr} + \frac{rf}{\Lambda}\partial_t Q^{tt}\right],$$

$$h_{tt}(t,r) = f^2 h_{rr} + f Q^{\sharp},$$

where

$$A(r) \equiv \frac{1}{r\Lambda}\left[\lambda(\lambda+1) + \frac{3M}{r}\left(\lambda + \frac{2M}{r}\right)\right], \qquad B(r) \equiv \frac{1}{rf\Lambda}\left[\lambda\left(1 - \frac{3M}{r}\right) - \frac{3M^2}{r^2}\right]. \tag{5.6}$$

These equations result from the definition (C6) of Ψ_{even} and its substitution into the even-parity field equations (C3). The even-parity projections of the stress-energy tensor that appear in the equations above are defined by Eqs. (C4). By enforcing the delta function constraints, they can be written in fully evaluated form (see App. B), with each having a time dependent magnitude multiplying the radial delta function

$$Q^{ab}(t,r) \equiv q^{ab}(t)\,\delta[r - r_p(t)], \qquad Q^a(t,r) \equiv q^a(t)\,\delta[r - r_p(t)],$$

$$Q^{\flat}(t,r) \equiv q^{\flat}(t)\,\delta[r - r_p(t)], \qquad Q^{\sharp}(t,r) \equiv q^{\sharp}(t)\,\delta[r - r_p(t)], \tag{5.7}$$

where we use a lowercase q as the base symbol of the corresponding magnitude. With Eq. (2.4) giving the four-velocity u^{μ}, the stress-energy tensor and Eqs. (C4) can be used to find

$$q^{tt}(t) = 8\pi\mu\frac{\mathcal{E}}{r_p^2 f_p}Y^*, \qquad q^{rr}(t) = 8\pi\mu\frac{f_p}{\mathcal{E}r_p^2}\left(\mathcal{E}^2 - U_p^2\right)Y^*, \qquad q^{tr}(t) = 8\pi\mu\frac{u^r}{r_p^2}Y^*,$$

$$q^t(t) = \frac{16\pi\mu}{\ell(\ell+1)}\frac{\mathcal{L}}{r_p^2}Y_{\varphi}^*, \qquad q^r(t) = \frac{16\pi\mu}{\ell(\ell+1)}\frac{\mathcal{L}}{\mathcal{E}}\frac{f_p}{r_p^2}u^r Y_{\varphi}^*, \tag{5.8}$$

$$q^{\flat}(t) = 8\pi\mu\frac{\mathcal{L}^2}{\mathcal{E}}\frac{f_p}{r_p^4}Y^*, \qquad q^{\sharp}(t) = 32\pi\mu\frac{(\ell-2)!}{(\ell+2)!}\frac{\mathcal{L}^2}{\mathcal{E}}\frac{f_p}{r_p^2}Y_{\varphi\varphi}^*.$$

Here, Y, Y_{φ}, and $Y_{\varphi\varphi}$ are shorthand for the even-parity scalar, vector, and tensor spherical harmonics, respectively, evaluated along the worldline at $\theta = \pi/2$ and $\varphi = \varphi_p(t)$.

Now consider the reconstruction of the MP amplitude K, given in Eq. (5.5). Using the expected functional form of Ψ given in Eq. (1.2), K obviously does fit the general form (5.1) claimed above. In fact, we find

$$K^{\pm}(t,r) = f\partial_r\Psi^{\pm} + A\Psi^{\pm}, \qquad K^S(t) = f_p[\![\Psi]\!]_p - \frac{r_p^2 f_p^2}{(\lambda+1)\Lambda_p}q^{tt} = 0, \tag{5.9}$$

where the vanishing of K^S follows from use of Eq. (3.11) for $[\![\Psi]\!]_p$, and q^{tt} from Eq. (5.8). Therefore, we see that the even-parity metric function K in Regge-Wheeler gauge is (only) a C^{-1} function at the location of the particle.

Using the same approach to evaluate h_{rr} in Eq. (5.5) we have

$$h_{rr}^{\pm}(t,r) = \frac{\Lambda}{f^2}\left[\frac{\lambda+1}{r}\Psi^{\pm} - K^{\pm}\right] + \frac{r}{f}\partial_r K^{\pm}, \qquad h_{rr}^S(t) = \frac{r_p}{f_p}[\![K]\!]_p = r_p[\![\partial_r\Psi]\!]_p + \frac{r_p A_p}{f_p}[\![\Psi]\!]_p. \tag{5.10}$$

Here, we have extended in a natural way the use of the $[\![\ ]\!]_p$ notation to let $[\![K]\!]_p$ represent the jump in K at $z = 0$. We find that the Regge-Wheeler metric function h_{rr} is not only discontinuous across $r_p(t)$ but also has a point-singular term, which is an artifact of Regge-Wheeler gauge.

The h_{tr} function is more subtle than the previous two. Looking at Eq. (5.5), we need the following terms involving Ψ,

$$rB\,\partial_t\Psi = rB\,\partial_t\Psi^+\,\theta(z) + rB\,\partial_t\Psi^-\,\theta(-z) - r_p B_p \dot{r}_p [\![\Psi]\!]_p\,\delta(z),$$

$$r\partial_t\partial_r\Psi = r\partial_t\partial_r\Psi^+\theta(z) + r\partial_t\partial_r\Psi^-\theta(-z) + \left[r_p\frac{d}{dt}\big([\![\Psi]\!]_p\big) + \dot{r}_p[\![\Psi]\!]_p - r_p\dot{r}_p[\![\partial_r\Psi]\!]_p\right]\delta(z) - r_p\dot{r}_p[\![\Psi]\!]_p\,\delta'(z).$$

(5.11)

On the right side of these equations we have evaluated all the δ and δ' coefficients at $z = 0$ with Eqs. (A1) and (A5) (fully evaluated form). The singular terms that arise in these expressions can be grouped with the similarly singular contributions from the source terms,

$$\frac{r^2}{\lambda+1}Q^{tr} = \frac{r_p^2}{\lambda+1}q^{tr}\delta(z),$$

$$\frac{r^3 f}{(\lambda+1)\Lambda}\partial_t Q^{tt} = \frac{1}{(\lambda+1)\Lambda_p}\left[r_p^3 f_p\frac{dq^{tt}}{dt} + \frac{3\lambda r_p^2 + 12Mr_p - 4\lambda Mr_p - 18M^2}{\Lambda_p}\dot{r}_p q^{tt}\right]\delta(z) - \frac{r_p^3 f_p}{(\lambda+1)\Lambda_p}\dot{r}_p q^{tt}\,\delta'(z).$$

(5.12)

Upon carefully checking the time dependence of q^{tt} and the jump in Ψ, we find that the δ' terms cancel out. There are multiple δ terms, but after using the expressions for $[\![\Psi]\!]_p$, $[\![\partial_r\Psi]\!]_p$ in (3.11) and the relevant q's in (5.8), most of the terms cancel and we are left with

$$h_{tr}^\pm(t,r) = r\partial_t\partial_r\Psi^\pm + rB\,\partial_t\Psi^\pm, \qquad h_{tr}^S(t) = \mathcal{E}^2\frac{\dot{r}_p}{f_p U_p^2}q^\sharp.$$

(5.13)

Finally, the h_{tt} term is simple. We insert Eq. (5.10) into the field equation for h_{tt} and get

$$h_{tt}^\pm(t,r) = f^2 h_{rr}^\pm, \qquad h_{tt}^S(t) = f_p^2 h_{rr}^S + f_p q^\sharp.$$

(5.14)

So, we see that in Regge-Wheeler gauge K is C^{-1} with no singularity along the worldline of the particle, but the three even-parity MP amplitudes in the "t, r sector" have point-singular artifacts given by Eqs. (5.10), (5.13), (5.14).

B. Odd parity

Once $\Psi_{\rm odd}$ has been computed, the odd-parity MP amplitudes can be reconstructed via

$$h_t(t,r) = \frac{f}{2}\partial_r\left(r\Psi_{\rm odd}\right) - \frac{r^2 f}{2\lambda}P^t, \qquad h_r(t,r) = \frac{r}{2f}\partial_t\Psi_{\rm odd} + \frac{r^2}{2\lambda f}P^r,$$

(5.15)

(see [31]). These equations follow from the definition (C14) and its substitution into the odd-parity field equations (C11). Similar to before, we define the lowercase p's to be the time-dependent magnitudes of the radial delta function after fully evaluating the odd-parity projections of the stress-energy tensor

$$P^a(t,r) \equiv p^a(t)\,\delta[r - r_p(t)], \qquad P(t,r) \equiv p(t)\,\delta[r - r_p(t)].$$

(5.16)

Also as before, we use the time dependence of the four-velocity and the stress-energy tensor to determine these magnitudes for eccentric motion on Schwarzschild,

$$p^t(t) = \frac{16\pi\mu}{\ell(\ell+1)}\frac{\mathcal{L}}{r_p^2}X_\varphi^*, \qquad p^r(t) = \frac{16\pi\mu}{\ell(\ell+1)}\frac{\mathcal{L}}{\mathcal{E}}\frac{f_p}{r_p^2}u^r X_\varphi^*, \qquad p(t) = 16\pi\mu\frac{(\ell-2)!}{(\ell+2)!}\frac{\mathcal{L}^2}{\mathcal{E}}\frac{f_p}{r_p^2}X_{\varphi\varphi}^*.$$

(5.17)

Here, X_φ and $X_{\varphi\varphi}$ are shorthand for the odd-parity vector and tensor spherical harmonics evaluated along the worldline at $\theta = \pi/2$ and $\varphi = \varphi_p(t)$.

Now, as in the even-parity case we can analyze the local structure of the MP amplitudes. We again assume Ψ to have the form Eq. (1.2). Plugging the relevant expressions into Eq. (5.15) for the odd-parity MP amplitude reconstruction, we find that all the point-singular parts cancel out exactly, leaving

$$h_t^\pm(t,r) = \frac{f}{2}\partial_r\left(r\Psi^\pm\right), \qquad h_t^S(t) = 0,$$

$$h_r^\pm(t,r) = \frac{r}{2f}\partial_t\Psi^\pm, \qquad h_r^S(t) = 0.$$

(5.18)

So, we see that the odd-parity MP functions in Regge-Wheeler gauge are smooth as they approach $r_p(t)$ with only a finite jump at that point.

FIG. 5 summarizes these findings graphically, for both even and odd parity, using several specific spherical harmonic modes.
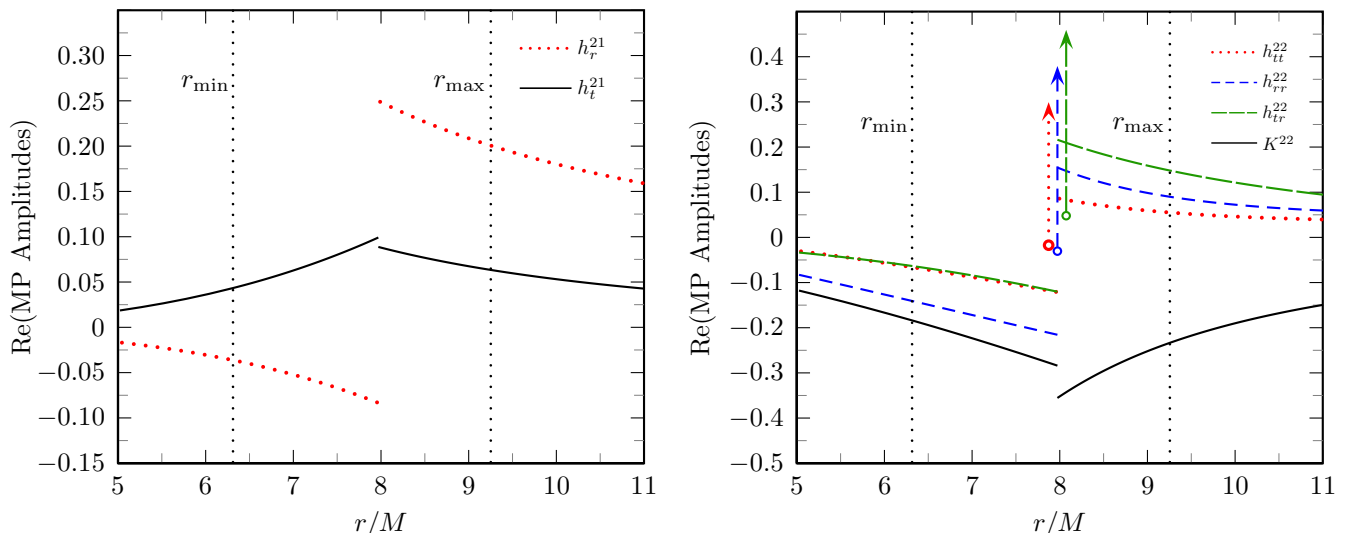
FIG. 5: The EHS approach to reconstructing the TD MP amplitudes. We consider a particle orbiting with $p = 7.50478$ and $e = 0.188917$ at $t = 80.62M$. The left plot shows the odd-parity MP amplitudes h_r^{21} and h_t^{21}. The right shows the even-parity h_{tt}^{22}, h_{rr}^{22}, h_{tr}^{22}, and K^{22}. Note that the amplitudes h_{tt}^{22}, h_{rr}^{22}, and h_{tr}^{22} are singular along the particle's worldline, as indicated by arrows in the plot on the right. The magnitude of these singularities are given in Eqs. (5.10), (5.13), (5.14). The remaining three MP amplitudes approach the particle location smoothly, and have only a finite jump at that point.

VI. CONCLUSION

We have achieved two main results with this paper. First, we have shown successful application of the method of extended homogeneous solutions to gravitational perturbations from a small mass in eccentric orbit about a massive Schwarzschild black hole. In doing so, we accurately computed the master functions in the Regge-Wheeler-Zerilli formalism in the frequency domain and transformed these fields back to the time domain. With this method we achieved exponential convergence of the master functions and their derivatives for all r including the instantaneous particle location $r = r_p(t)$.

Our second important result is the reconstruction of the metric perturbation amplitudes in Regge-Wheeler gauge for arbitrary radiative modes. In addition to computing the smooth parts of these amplitudes, we have derived the time dependent magnitudes of point-singular terms that reside at $r_p(t)$ in some components of the metric. This full and accurate knowledge of the spherical harmonic amplitudes of the metric at, and near, $r_p(t)$ lays the groundwork for one or more subsequent approaches to local computation of the self-force.

Acknowledgments

Appendix A: The fully evaluated form of distributional source terms

In the RWZ formalism for perturbations generated by an orbiting point mass, the master equations have distributional sources with both delta function and derivative-of-delta function terms. Reduced by spherical harmonic decomposition, these distributions have support only along a one-dimensional timelike worldline $r = r_p(t)$ within a two dimensional domain. The delta function's behavior is still elementary,

$$\alpha(t,r)\,\delta[r - r_p(t)] = \alpha\,(t, r_p(t))\,\delta[r - r_p(t)] \equiv \tilde{\alpha}(t)\,\delta[r - r_p(t)], \tag{A1}$$

where $\alpha(t,r)$ is assumed to be a smooth function and we use the notation $\tilde{\alpha}(t)$ to indicate the one-dimensional function that results from restricting (or fully evaluating) $\alpha(t,r)$ with the delta function. At any stage in a calculation a delta function can be used to fully evaluate all smooth functions that multiply it. Under an integral the result is obvious

$$\int \alpha(t,r)\,\delta[r-r_p(t)]\,dr = \tilde{\alpha}(t), \tag{A2}$$

with the resulting function of time being unique. Occasionally, there is need to differentiate such a function. The total derivative is related to derivatives of the original function by

$$\frac{d\tilde{\alpha}}{dt} = \Big[\partial_t\alpha(t,r) + \dot{r}_p\partial_r\alpha(t,r)\Big]_{r=r_p(t)}, \tag{A3}$$

where on the right hand side we differentiate first and evaluate second.

Of more interest is the behavior of δ' [40]. Differentiating Eq. (A1) with respect to r, we obtain

$$\alpha(t,r)\,\delta'[r-r_p(t)] + \partial_r\alpha(t,r)\,\delta[r-r_p(t)] = \tilde{\alpha}(t)\,\delta'[r-r_p(t)]. \tag{A4}$$

Rearranging terms and using the rule of fully evaluating whenever possible, we find

$$\alpha(t,r)\,\delta'[r-r_p(t)] = \tilde{\alpha}(t)\,\delta'[r-r_p(t)] - \tilde{\beta}(t)\,\delta[r-r_p(t)], \qquad \tilde{\beta}(t) \equiv \partial_r\alpha(t,r_p(t)) \equiv \Big[\partial_r\alpha(t,r)\Big]_{r=r_p(t)}, \tag{A5}$$

which is the analogous fully evaluated form. Upon integration,

$$\int \alpha(t,r)\,\delta'[r-r_p(t)]\,dr = -\tilde{\beta}(t) = -\partial_r\alpha(t,r_p(t)). \tag{A6}$$

Since the first term on the right of Eq. (A5) disappears upon integration, why retain it? The answer is that we may multiply Eq. (A5) by another smooth (test) function, $\gamma(t,r)$. We can then proceed to fully evaluated form by reducing the smooth function $\gamma(t,r)\,\alpha(t,r)$ on the left or use the same reduction on the first term on the right. In either case the result is

$$\gamma(t,r)\,\alpha(t,r)\,\delta'[r-r_p(t)] = \tilde{\gamma}(t)\,\tilde{\alpha}(t)\,\delta'[r-r_p(t)] - \tilde{\alpha}(t)\,\partial_r\gamma(t,r_p(t))\,\delta[r-r_p(t)] - \tilde{\gamma}(t)\,\partial_r\alpha(t,r_p(t))\,\delta[r-r_p(t)]. \tag{A7}$$

From this it is evident that we can *partially* evaluate a coefficient of δ' in a number of different ways.

Martel [30] introduced the notation found in Eq. (1.1) for gravitational master function source terms, with two-dimensional functions $G_{\ell m}(t,r)$ and $F_{\ell m}(t,r)$ multiplying δ and δ', respectively. In examining the Zerilli-Moncrief master function, he left these coefficients partially evaluated. Sopuerta and Laguna [35] started with the same notation for $G_{\ell m}(t,r)$ and $F_{\ell m}(t,r)$ in the case of the Cunningham-Price-Moncrief master function, and fully evaluated these coefficients at $r=r_p(t)$. A difficulty with the $G_{\ell m}(t,r)$ and $F_{\ell m}(t,r)$ notation is that there is no unique form of these functions if partially evaluated. Any solution of the RWZ wave equation will require a full evaluation of the source. The procedure should not matter but we prefer the clarity afforded by using the identities found in Eqs. (A1) and (A5) to write Eq. (1.1) in fully evaluated form from the outset

$$S_{\ell m}(t,r) = \tilde{G}_{\ell m}(t)\,\delta[r-r_p(t)] + \tilde{F}_{\ell m}(t)\,\delta'[r-r_p(t)], \tag{A8}$$

where

$$\tilde{G}_{\ell m}(t) \equiv \Big[G_{\ell m}(t,r) - \partial_r F_{\ell m}(t,r)\Big]_{r=r_p(t)}, \qquad \tilde{F}_{\ell m}(t) \equiv \Big[F_{\ell m}(t,r)\Big]_{r=r_p(t)}. \tag{A9}$$

Appendix B: Source terms for eccentric motion on Schwarzschild

Here we give the unambiguous expressions for $\tilde{G}_{\ell m}$ and $\tilde{F}_{\ell m}$ for the even-parity Zerilli-Moncrief and odd-parity Cunningham-Price-Moncrief master functions fully evaluated at $r=r_p(t)$. We introduce new notation for constituent parts of $\tilde{G}_{\ell m}$ and $\tilde{F}_{\ell m}$ based upon the projections of the stress-energy tensor defined in App. C and the fully evaluated time-dependent magnitudes of $\delta[r-r_p(t)]$ given by Eqs. (5.8) and (5.17). Note that we use $\mathcal{G}$ and $\mathcal{F}$ to denote additional time-dependent factors that multiply the various stress-energy magnitudes. The indices on these $\mathcal{G}$ and $\mathcal{F}$ factors are not tensor indices.

1. Even parity

In the even-parity case, we examine the terms first published by Martel [30], but now fully evaluate them at $r = r_p(t)$. We find,

$$\tilde{G}_{\ell m}(t) = \mathcal{G}_\ell^{rr}\, q_{\ell m}^{rr} + \mathcal{G}_\ell^{tt}\, q_{\ell m}^{tt} + \mathcal{G}_\ell^r\, q_{\ell m}^r + \mathcal{G}_\ell^\flat\, q_{\ell m}^\flat + \mathcal{G}_\ell^\sharp\, q_{\ell m}^\sharp$$
$$\tilde{F}_{\ell m}(t) = \mathcal{F}_\ell^{rr}\, q_{\ell m}^{rr} + \mathcal{F}_\ell^{tt}\, q_{\ell m}^{tt}, \tag{B1}$$

where

$$\mathcal{G}_\ell^{rr}(t) \equiv \frac{1}{(\lambda+1)\, r_p \Lambda_p^2}\Big[(\lambda+1)\,(\lambda r_p + 6M)\, r_p + 3M^2 \Big],$$

$$\mathcal{G}_\ell^{tt}(t) \equiv -\frac{f_p^2}{(\lambda+1) r_p \Lambda_p^2}\Big[\lambda\,(\lambda+1)\, r_p^2 + 6\lambda M r_p + 15M^2 \Big],$$

$$\mathcal{G}_\ell^r(t) \equiv \frac{2 f_p}{\Lambda_p}, \qquad \mathcal{G}_\ell^\flat(t) \equiv \frac{r_p f_p^2}{(\lambda+1)\Lambda_p}, \qquad \mathcal{G}_\ell^\sharp(t) \equiv -\frac{f_p}{r_p}, \tag{B2}$$

$$\mathcal{F}_\ell^{rr}(t) \equiv -\frac{r_p^2 f_p}{(\lambda+1)\,\Lambda_p}, \qquad \mathcal{F}_\ell^{tt}(t) \equiv \frac{r_p^2 f_p^3}{(\lambda+1)\,\Lambda_p},$$

with the q's given in Eq. (5.8).

2. Odd parity

In the odd-parity case, the fully evaluated source magnitudes are equivalent to those first published by Sopuerta and Laguna [35] and later with more detail by Field, Hesthaven, and Lau [44]. We find,

$$\tilde{G}_{\ell m}(t) = \mathcal{G}_\ell^{r_1}\, p_{\ell m}^r + \mathcal{G}_\ell^{r_2}\, \frac{dp_{\ell m}^r}{dt} + \mathcal{G}_\ell^t\, p_{\ell m}^t, \qquad \tilde{F}_{\ell m}(t) = \mathcal{F}_\ell^r\, p_{\ell m}^r + \mathcal{F}_\ell^t\, p_{\ell m}^t, \tag{B3}$$

where

$$\mathcal{G}_\ell^{r_1}(t) \equiv \frac{\dot{r}_p}{\lambda}, \qquad \mathcal{G}_\ell^{r_2}(t) \equiv \frac{r_p}{\lambda}, \qquad \mathcal{G}_\ell^t(t) \equiv -\frac{f_p}{\lambda}, \qquad \mathcal{F}_\ell^r(t) \equiv -\frac{r_p \dot{r}_p}{\lambda}, \qquad \mathcal{F}_\ell^t(t) \equiv \frac{r_p f_p^2}{\lambda}, \tag{B4}$$

and the p's are given by Eq. (5.17).

Appendix C: Metric perturbation formalism in the Regge-Wheeler gauge

Here we briefly summarize the definitions of metric perturbation (MP) amplitudes (on a common tensor spherical harmonic basis) for both even and odd parities. The field equations and Bianchi identities are given in terms of the MP amplitudes and spherical harmonic projected source terms. The specific gauge invariant master functions we use in our simulations are expressed in terms of the MP amplitudes and their associated master equations, potentials, and source terms are summarized. In what follows, lowercase Latin indices will run over (t, r), while uppercase Latin indices will run over (θ, φ). This section draws heavily from Martel and Poisson [25]. The material here serves as a basis for discussing in Sec. V how the MP can be numerically reconstructed from the master functions.

1. Even parity

Of the ten MP amplitudes, seven are in the even-parity sector. Using the decomposition of Martel and Poisson [25], they are

$$p_{ab}\left(x^\mu\right) = \sum_{\ell,m} h_{ab}^{\ell m} Y^{\ell m}, \qquad p_{aB}\left(x^\mu\right) = \sum_{\ell,m} j_a^{\ell m} Y_B^{\ell m}, \qquad p_{AB}\left(x^\mu\right) = r^2 \sum_{\ell,m} \left(K^{\ell m}\Omega_{AB}Y^{\ell m} + G^{\ell m}Y_{AB}^{\ell m} \right). \tag{C1}$$

The tensor Ω_{AB} is the metric on the unit two-sphere,

$$ds^2 = \Omega_{AB}dx^A dx^B = d\theta^2 + \sin^2\theta \, d\varphi^2. \tag{C2}$$

The even-parity scalar $(Y^{\ell m})$, vector $(Y_A^{\ell m})$, and tensor $(Y_{AB}^{\ell m}$ and $\Omega_{AB}Y^{\ell m})$ spherical harmonics are defined in [25]. Note that $Y_{AB}^{\ell m}$ is the trace-free tensor spherical harmonic, which differs from what Regge and Wheeler used in their original work [19]. For the remainder of this section, we drop ℓ and m indices for the sake of brevity.

In Schwarzschild coordinates, the amplitudes defined here are related to Regge and Wheeler's original quantities. In the "t, r sector," $h_{tt} = fH_0$, $h_{tr} = H_1$, and $h_{rr} = H_2/f$. For the off-diagonal elements, $j_t = h_0$ and $j_r = h_1$. Finally, on the two-sphere $G_{\text{here}} = G_{\text{RW}}$, while $K_{\text{here}} = K_{\text{RW}} - \ell(\ell+1)G/2$. We use the Regge-Wheeler gauge, where $j_a = G = 0$. In this gauge and in Schwarzschild coordinates, the even-parity field equations are

$$-\partial_r^2 K - \frac{3r-5M}{r^2 f}\partial_r K + \frac{f}{r}\partial_r h_{rr} + \frac{(\lambda+2)\,r+2M}{r^3}h_{rr} + \frac{\lambda}{r^2 f}K = Q^{tt},$$

$$\partial_t \partial_r K + \frac{r-3M}{r^2 f}\partial_t K - \frac{f}{r}\partial_t h_{rr} - \frac{\lambda+1}{r^2}h_{tr} = Q^{tr},$$

$$-\partial_t^2 K + \frac{(r-M)f}{r^2}\partial_r K + \frac{2f}{r}\partial_t h_{tr} - \frac{f}{r}\partial_r h_{tt} + \frac{(\lambda+1)r+2M}{r^3}h_{tt} - \frac{f^2}{r^2}h_{rr} - \frac{\lambda f}{r^2}K = Q^{rr},$$

$$\partial_t h_{rr} - \partial_r h_{tr} + \frac{1}{f}\partial_t K - \frac{2M}{r^2 f}h_{tr} = Q^t,$$

$$-\partial_t h_{tr} + \partial_r h_{tt} - f\partial_r K - \frac{r-M}{r^2 f}h_{tt} + \frac{(r-M)f}{r^2}h_{rr} = Q^r, \tag{C3}$$

$$-\partial_t^2 h_{rr} + 2\partial_t\partial_r h_{tr} - \partial_r^2 h_{tt} - \frac{1}{f}\partial_t^2 K + f\partial_r^2 K + \frac{2(r-M)}{r^2 f}\partial_t h_{tr} - \frac{r-3M}{r^2 f}\partial_r h_{tt} - \frac{(r-M)f}{r^2}\partial_r h_{rr}$$

$$+\frac{2(r-M)}{r^2}\partial_r K + \frac{(\lambda+1)r^2 - 2(\lambda+2)Mr + 2M^2}{r^4 f^2}h_{tt} - \frac{(\lambda+1)r^2 - 2\lambda Mr - 2M^2}{r^4}h_{rr} = Q^\flat,$$

$$\frac{1}{f}h_{tt} - fh_{rr} = Q^\sharp,$$

which rely upon the following source terms

$$Q^{ab}(t,r) \equiv 8\pi \int T^{ab}Y^* \, d\Omega, \qquad Q^a(t,r) \equiv \frac{16\pi r^2}{\ell(\ell+1)}\int T^{aB}Y_B^* \, d\Omega,$$

$$Q^\flat(t,r) \equiv 8\pi r^2 \int T^{AB}\Omega_{AB}Y^* \, d\Omega, \qquad Q^\sharp(t,r) \equiv 32\pi r^4 \frac{(\ell-2)!}{(\ell+2)!}\int T^{AB}Y_{AB}^* \, d\Omega. \tag{C4}$$

The conservation (Bianchi) identities are

$$\partial_t Q^{tt} + \partial_r Q^{tr} + 2\frac{(r-M)}{r^2 f}Q^{tr} - \frac{\lambda+1}{r^2}Q^t = 0,$$

$$\partial_t Q^{tr} + \partial_r Q^{rr} + \frac{Mf}{r^2}Q^{tt} + \frac{2r-5M}{r^2 f}Q^{rr} - \frac{\lambda+1}{r^2}Q^r - \frac{f}{r}Q^\flat = 0, \tag{C5}$$

$$\partial_t Q^t + \partial_r Q^r + \frac{2}{r}Q^r + Q^\flat - \frac{\lambda}{r^2}Q^\sharp = 0.$$

We use the gauge invariant *Zerilli-Moncrief* master function (see [22, 24], modifying the approach of [20]), which is

$$\Psi_{\text{even}}(t,r) \equiv \frac{2r}{\ell(\ell+1)}\left[K + \frac{1}{\Lambda}\left(f^2 h_{rr} - rf\partial_r K\right)\right], \tag{C6}$$

in Schwarzschild coordinates. It satisfies the wave equation

$$\left[-\frac{\partial^2}{\partial t^2} + \frac{\partial^2}{\partial r_*^2} - V_{\text{even}}\right]\Psi_{\text{even}} = S_{\text{even}}, \tag{C7}$$

with source term

$$S_{\text{even}}(t,r) \equiv \frac{1}{(\lambda+1)\Lambda}\left[r^2 f\left(f^2\partial_r Q^{tt} - \partial_r Q^{rr}\right) + r(\Lambda - f)Q^{rr} + rf^2 Q^\flat\right.$$

$$\left. - \frac{f^2}{r\Lambda}\left(\lambda(\lambda-1)r^2 + (4\lambda-9)\,Mr + 15M^2\right)Q^{tt}\right] + \frac{2f}{\Lambda}Q^r - \frac{f}{r}Q^\sharp, \tag{C8}$$

and standard Zerilli potential

$$V_{\text{even}}(r) \equiv \frac{f}{r^2\Lambda^2}\left[2\lambda^2\left(\lambda+1+\frac{3M}{r}\right)+\frac{18M^2}{r^2}\left(\lambda+\frac{M}{r}\right)\right]. \tag{C9}$$

2. Odd parity

The remaining three MP amplitudes belong to the odd-parity sector,

$$p_{ab}\left(x^\mu\right)=0, \qquad p_{aB}\left(x^\mu\right)=\sum_{\ell,m}h_a^{\ell m}X_B^{\ell m}, \qquad p_{AB}\left(x^\mu\right)=\sum_{\ell,m}h_2^{\ell m}X_{AB}^{\ell m}. \tag{C10}$$

The vector $(X_B^{\ell m})$ and tensor $(X_{AB}^{\ell m})$ spherical harmonics are those defined in [25]. Note that the tensor spherical harmonics differ from those used by Regge and Wheeler by a minus sign. For the remainder of this section, we again drop ℓ and m indices.

These MP amplitudes are related to Regge and Wheeler's quantities through $h_t = h_0$, $h_r = h_1$, and $h_2^{\text{here}} = -h_2^{\text{RW}}$. We use Regge-Wheeler gauge, in which $h_2 = 0$. In this gauge and in Schwarzschild coordinates, the odd-parity field equations are

$$-\partial_t\partial_r h_r + \partial_r^2 h_t - \frac{2}{r}\partial_t h_r - \frac{2(\lambda+1)r-4M}{r^3 f}h_t = P^t,$$

$$\partial_t^2 h_r - \partial_t\partial_r h_t + \frac{2}{r}\partial_t h_t + \frac{2\lambda f}{r^2}h_r = P^r, \tag{C11}$$

$$-\frac{1}{f}\partial_t h_t + f\partial_r h_r + \frac{2M}{r^2}h_r = P,$$

with source terms given by

$$P^a(t,r) \equiv \frac{16\pi r^2}{\ell(\ell+1)}\int T^{aB}X_B^* \, d\Omega, \qquad P(t,r) \equiv 16\pi r^4\frac{(\ell-2)!}{(\ell+2)!}\int T^{AB}X_{AB}^* \, d\Omega. \tag{C12}$$

The conservation (Bianchi) identity is

$$\partial_t P^t + \partial_r P^r + \frac{2}{r}P^r - \frac{2\lambda}{r^2}P = 0. \tag{C13}$$

In the odd-parity sector, we use the gauge-invariant *Cunningham-Price-Moncrief* master function [23], which in Schwarzschild coordinates is

$$\Psi_{\text{odd}}(t,r) \equiv \frac{r}{\lambda}\left[\partial_r h_t - \partial_t h_r - \frac{2}{r}h_t\right]. \tag{C14}$$

It satisfies the wave equation

$$\left[-\frac{\partial^2}{\partial t^2}+\frac{\partial^2}{\partial r_*^2}-V_{\text{odd}}\right]\Psi_{\text{odd}} = S_{\text{odd}}, \tag{C15}$$

with source term

$$S_{\text{odd}}(t,r) \equiv \frac{rf}{\lambda}\left[\frac{1}{f}\partial_t P^r + f\partial_r P^t + \frac{2M}{r^2}P^t\right], \tag{C16}$$

and standard Regge-Wheeler potential

$$V_{\text{odd}}(r) \equiv \frac{f}{r^2}\left[\ell\left(\ell+1\right)-\frac{6M}{r}\right]. \tag{C17}$$

Appendix D: Asymptotic expansions for Jost functions at $r_* \to \infty$

We examine here the asymptotic expansions that we use to set boundary conditions far from the black hole. The unit normalized solution to Eq. (2.16) is factored into the form

$$\hat{R}^+_{\ell mn}(r) = J^+_{\ell mn}(r)e^{i\omega_{mn}r_*}, \tag{D1}$$

where $J^+_{\ell mn}$ is the "Jost function" [27], which goes to 1 as $r_* \to +\infty$. (We can similarly define the horizon side Jost function through $\hat{R}^-_{\ell mn} = J^-_{\ell mn}e^{-i\omega_{mn}r_*}$, which goes to 1 as $r_* \to -\infty$.) Plugging this into the source free version of Eq. (2.16) and changing to r derivatives, we have

$$f\frac{d^2 J^+_{\ell mn}}{dr^2} + \left[\frac{2M}{r^2} + 2i\omega_{mn}\right]\frac{dJ^+_{\ell mn}}{dr} - \frac{V_\ell}{f}J^+_{\ell mn} = 0. \tag{D2}$$

From here we assume an asymptotic series solution of $J^+_{\ell mn}$ of the form

$$J^+_{\ell mn}(r) = \sum_{j=0}^{\infty} \frac{a_j}{(\omega_{mn}r)^j} \tag{D3}$$

Note that contrary to a Taylor expansion which converges for fixed r with increasing j, this series converges for fixed j with increasing r. When a specific potential is chosen, the method of Frobenius can be used to find the coefficients a_j. Plugging in the even-parity potential from Eq. (C9) a recurrence relation for the a_j is

$$2i\lambda^2 j\, a_j = \lambda\left[\lambda\,(j-1)\,j - 12i\sigma\,(j-1) - 2\lambda\,(\lambda+1)\right]a_{j-1}$$
$$+ 2\sigma\left[\lambda\,(3-\lambda)\,(j-2)\,(j-1) - \left(\lambda^2 + 9i\sigma\right)(j-2) - 3\lambda^2\right]a_{j-2}$$
$$+ 3\sigma^2\left[(3-4\lambda)\,(j-3)\,(j-2) - 4\lambda\,(j-3) - 6\lambda\right]a_{j-3} - 18\sigma^3\,(j-3)^2\,a_{j-4} \quad \text{(D4)}$$

where $\sigma \equiv M\omega_{mn}$. For the odd-parity expansion, we plug in the potential in Eq. (C17). The resulting recurrence relation is

$$2ij\, a_j = -2\sigma\left[(j+1)\,(j-3)\right]a_{j-2} - \left[\ell\,(\ell+1) - j\,(j-1)\right]a_{j-1}. \tag{D5}$$

In order to use these recurrence relations, the first few terms $a_0,\ a_1,\dots$ are needed. The recurrence relations actually provides them if one assumes that $a_j = 0$ for all negative j.

[1] ESA, *Esa science & technology: Lisa* (2010), `http://sci.esa.int/science-e/www/area/index.cfm?fareaid=27`.
[2] L. Barack, Class. Quant. Grav. **26**, 213001 (2009), 0908.1664.
[3] NASA, *Lisa - laser interferometer space antenna* (2010), `http://lisa.nasa.gov`.
[4] E. Poisson, Living Rev. Rel. **7**, 6 (2004), gr-qc/0306052.
[5] A. Pound, Phys. Rev. **D81**, 024023 (2010), 0907.5197.
[6] P. Dirac, Proc. R. Soc. London, Ser. A **167**, 148 (1938).
[7] Y. Mino, M. Sasaki, and T. Tanaka, Phys. Rev. D **55**, 3457 (1997).
[8] T. C. Quinn and R. M. Wald, Phys. Rev. D **56**, 3381 (1997).
[9] S. L. Detweiler and B. F. Whiting, Phys. Rev. **D67**, 024025 (2003), gr-qc/0202086.
[10] L. Barack and C. O. Lousto, Phys. Rev. D **66**, 061502 (2002).
[11] L. Barack and N. Sago, Phys. Rev. **D75**, 064021 (2007), gr-qc/0701069.
[12] S. Detweiler, Phys. Rev. **D77**, 124026 (2008), 0804.3529.
[13] L. Barack and N. Sago, Phys. Rev. Lett. **102**, 191101 (2009), 0902.0573.
[14] L. Barack and N. Sago (2010), 1002.2386.
[15] C. Cutler, D. Kennefick, and E. Poisson, Phys. Rev. D **50**, 3816 (1994).
[16] K. Glampedakis, S. A. Hughes, and D. Kennefick, Phys. Rev. **D66**, 064005 (2002), gr-qc/0205033.
[17] S. A. Hughes, S. Drasco, E. E. Flanagan, and J. Franklin, Phys. Rev. Lett. **94**, 221101 (2005), gr-qc/0504015.
[18] Y. Mino, Phys. Rev. **D67**, 084027 (2003), gr-qc/0302075.
[19] T. Regge and J. Wheeler, Phys. Rev. **108**, 1063 (1957).

[20] F. Zerilli, Phys. Rev. D **2**, 2141 (1970).
[21] C. Vishveshwara, Phys. Rev. D **1**, 2870 (1970).
[22] V. Moncrief, Ann. Phys. **88**, 323 (1974).
[23] C. Cunningham, R. Price, and V. Moncrief, Astrophys. J. **224**, 643 (1978).
[24] C. Cunningham, R. Price, and V. Moncrief, Astrophys. J. **230**, 870 (1979).
[25] K. Martel and E. Poisson, Phys. Rev. D **71**, 104003 (2005), arXiv:gr-qc/0502028.
[26] S. Teukolsky, Astrophys. J. **185**, 635 (1973).
[27] S. Chandrasekhar, *The Mathematical Theory of Black Holes*, vol. 69 of *The International Series of Monographs on Physics* (Clarendon, Oxford, 1983).
[28] M. Sasaki and H. Tagoshi, Living Reviews in Relativity **6** (2003).
[29] L. Barack and C. O. Lousto, Phys. Rev. **D72**, 104026 (2005), gr-qc/0510019.
[30] K. Martel, Physical Review D **69**, 044025 (2004).
[31] C. O. Lousto, Classical and Quantum Gravity **22**, S569 (2005).
[32] S. L. Detweiler and E. Poisson, Phys. Rev. **D69**, 084019 (2004), gr-qc/0312010.
[33] L. Barack and L. M. Burko, Phys. Rev. **D62**, 084040 (2000), gr-qc/0007033.
[34] R. Haas, Phys. Rev. **D75**, 124011 (2007), 0704.0797.
[35] C. F. Sopuerta and P. Laguna, Physical Review D **73**, 044028 (2006).
[36] L. M. Burko, Phys. Rev. Lett. **84**, 4529 (2000), gr-qc/0003074.
[37] S. Detweiler, E. Messaritaki, and B. F. Whiting, Phys. Rev. **D67**, 104016 (2003), gr-qc/0205079.
[38] L. Barack, A. Ori, and N. Sago, Phys. Rev. D **78**, 084021 (2008), 0808.2315.
[39] D. C. Champeney, *A Handbook of Fourier Theorems* (Cambridge University Press, 1989).
[40] M. J. Lighthill, *Fourier Analysis and Generalised Functions* (Cambridge University Press, 1958).
[41] C. Misner, K. Thorne, and J. Wheeler, *Gravitation* (Freeman, San Francisco, CA, U.S.A., 1973).
[42] C. Darwin, Proc. R. Soc. Lond. A **249**, 180 (1959).
[43] W. Schmidt, Class. Quant. Grav. **19**, 2743 (2002), gr-qc/0202090.
[44] S. E. Field, J. S. Hesthaven, and S. R. Lau, Class. Quant. Grav. **26**, 165010 (2009), 0902.1287.
[45] J. L. Barton, D. J. Lazar, D. J. Kennefick, G. Khanna, and L. M. Burko, Phys. Rev. **D78**, 064042 (2008), 0804.1075.
[46] D. V. Gal'tsov, Journal of Physics A: Mathematical and General **15**, 3737 (1982).
[47] S. Drasco, E. E. Flanagan, and S. A. Hughes, Classical and Quantum Gravity **22**, S801 (2005).
[48] W. H. Press, S. A. Teukolsky, W. T. Vetterling, and B. P. Flannery, *Numerical Recipes in C: The Art of Scientific Computing* (Cambridge University Press, Cambridge, UK, 1993), 2nd ed.
[49] K. S. Thorne, Rev. Mod. Phys. **52**, 299 (1980).
[50] C. Cutler, L. S. Finn, E. Poisson, and G. J. Sussman, Phys. Rev. D **47**, 1511 (1993).
[51] R. Fujita, W. Hikida, and H. Tagoshi, Prog. Theor. Phys. **121**, 843 (2009), 0904.3810.
[52] L. Barack and A. Ori, Phys. Rev. **D61**, 061502 (2000), gr-qc/9912010.